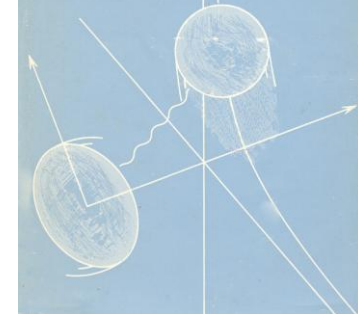


Coulomb excitation - a tool for nuclear shapes and more



- Introduction
- Theoretical aspects of Coulomb excitation
- Experimental considerations, set-ups and analysis techniques
- Recent highlights and future perspectives

Lecture given at the
Ecole Joliot Curie 2012
Wolfram KORTEN
CEA Saclay

Coulomb excitation - the different energy regimes

Low-energy regime ($< 5 \text{ MeV/u}$)

High-energy regime ($\gg 5 \text{ MeV/u}$)

Energy cut-off $\Delta E_{\text{max}} = \frac{\hbar v_{\infty}}{a \varepsilon} \approx 2 \text{ MeV}$ $\Delta E_{\text{max}} = \hbar c \frac{\beta \gamma}{a \varepsilon} \approx 10 \text{ MeV} (\beta = 0.4)$

Spin cut-off: L_{max} : up to $30\hbar$ mainly single-step excitations

Cross section: $d\sigma/d\theta \sim \langle I_i || M(\sigma\lambda) || I_f \rangle$ $\sigma_{\lambda} \sim (Z_p e^2 / \hbar c)^2 B(\sigma\lambda, 0 \rightarrow \lambda)$
 differential integral

Luminosity: **low** mg/cm^2 targets **high** g/cm^2 targets
 Beam intensity: **high** $>10^3$ pps **low** a few pps

**Comprehensive study of
low-lying excitations**

**First exploration of excited
states in very "exotic" nuclei**

Coulomb excitation with stable beams

I r f u

cea

saclay

Early experimental approach, until ~1970: light ion beams ($p, \alpha, ^{12}\text{C}, ^{16}\text{O}, \dots$)
Particle spectroscopy using spectrometers or Si detectors

Advantages:

Direct measurement of $P = \sigma / \sigma_{\text{ruth}}$

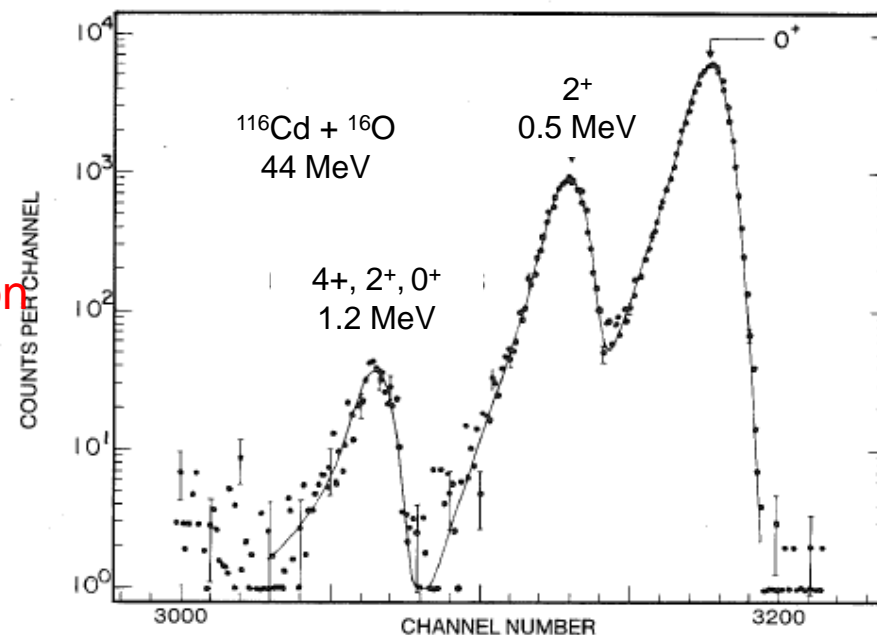
Disadvantages :

Si detectors have **limited energy resolution** (>100 keV), despite thin targets etc.

High-resolution spectrometers have very **limited angular coverage** \rightarrow angular scan

\rightarrow limitation to first excited state(s) and nuclei with low level density

Method limited to light beams ($\alpha, ^{12}\text{C}, ^{16}\text{O}, ^{20}\text{Ne}$)
since energy resolution scales with mass ($E/A \sim \text{const.}$)



Coulomb excitation with stable beams

1970/80: Particle-gamma coincidence spectroscopy using NaI and/or Ge detector arrays in conjunction with charged particle detectors

Advantages:

high resolution (few keV with Ge detectors) combined with high efficiency (close to 100% with NaI arrays)

Disadvantages :

Energy resolution limited by Doppler effect

→ high granularity for detection of both particle and gamma rays

Need to detect particle-gamma coincidences

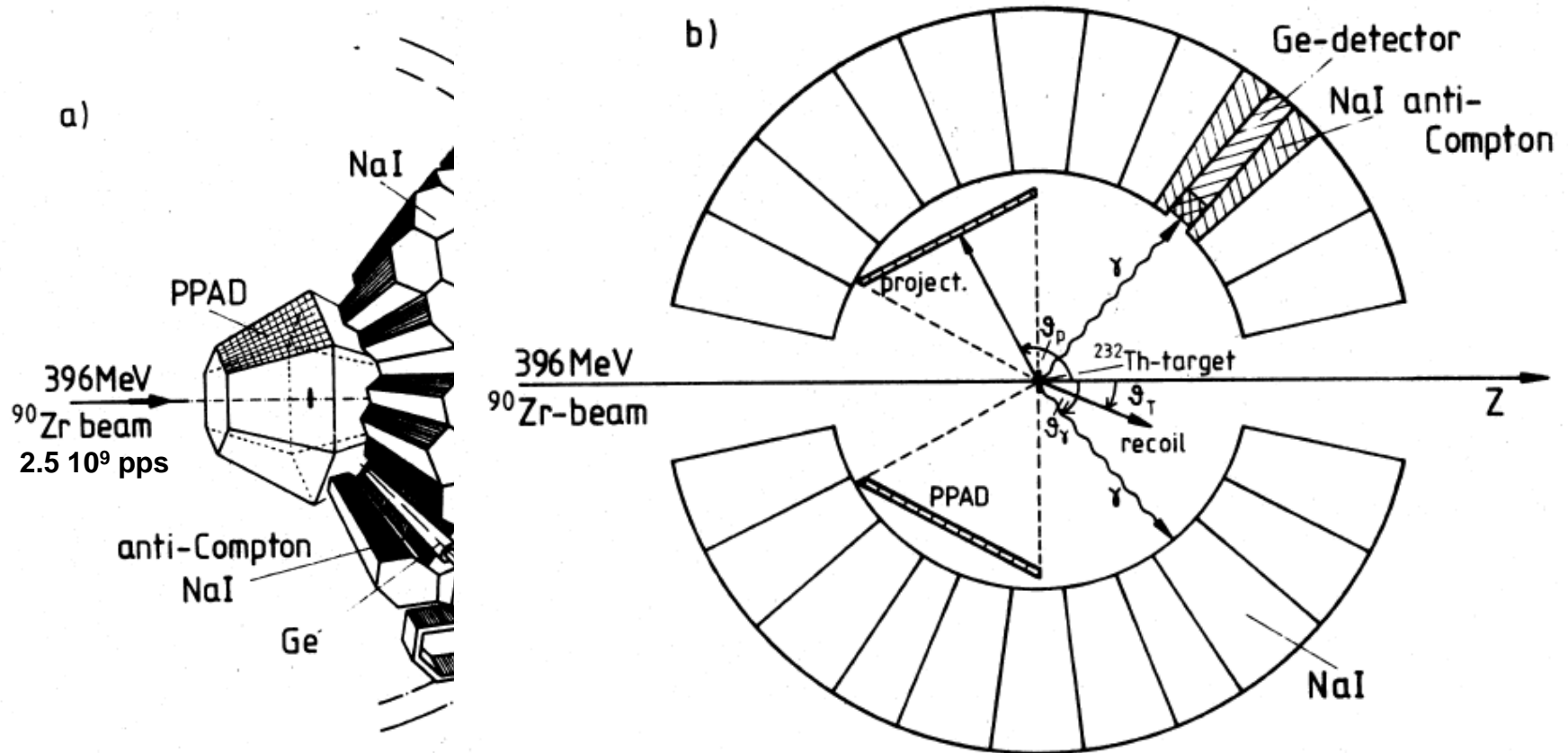
→ 4π arrays or reduced (coincidence) efficiency

Indirect measurement $Y_\gamma(I_i \rightarrow I_f) \rightarrow \sigma(I_i, \theta_{cm})$

→ need to take into account branching ratios, particle- γ angular distribution,

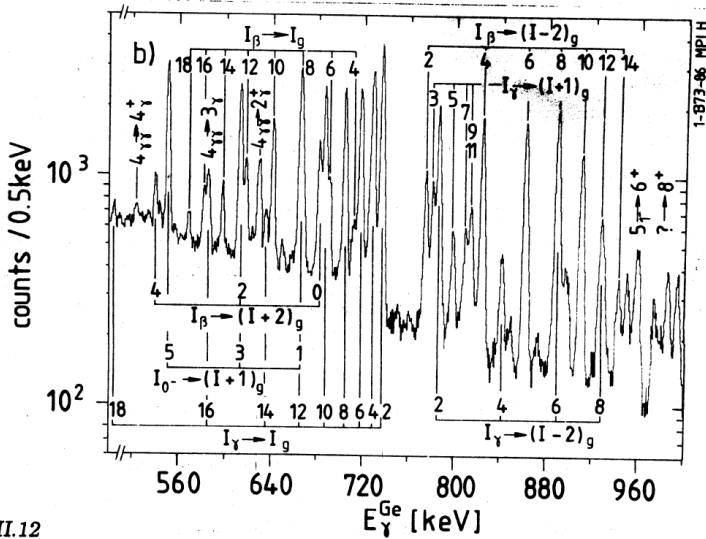
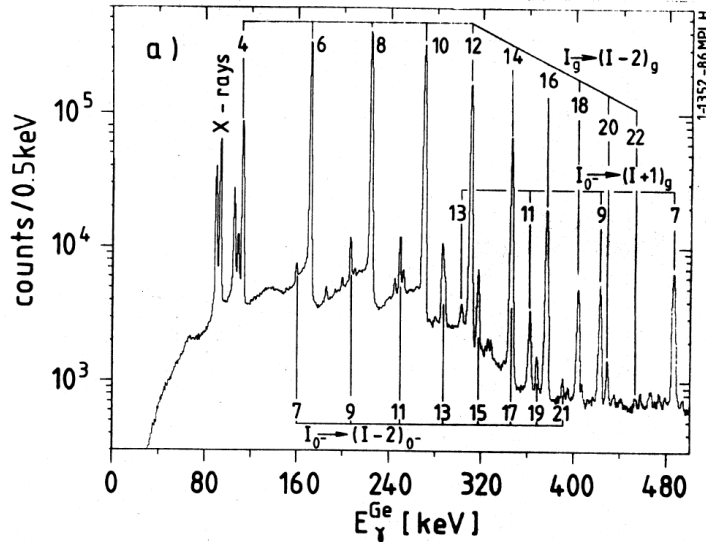
→ corrections needed for efficiencies, etc.

Experimental setup for multi-step Coulomb excitation experiments with stable beams



- Advantage: 4π array for both particles and γ rays ; good spatial resolution (few $^\circ$)
Identification of reaction partners through Time-of-Flight
- Limitation: low resolution for NaI scintillators,
low efficiency for Ge detectors ($\sim 0.5\%$) due to large distance ($\sim 25\text{cm}$)

Example for a multi-step Coulomb excitation experiment with a stable heavy ion beam

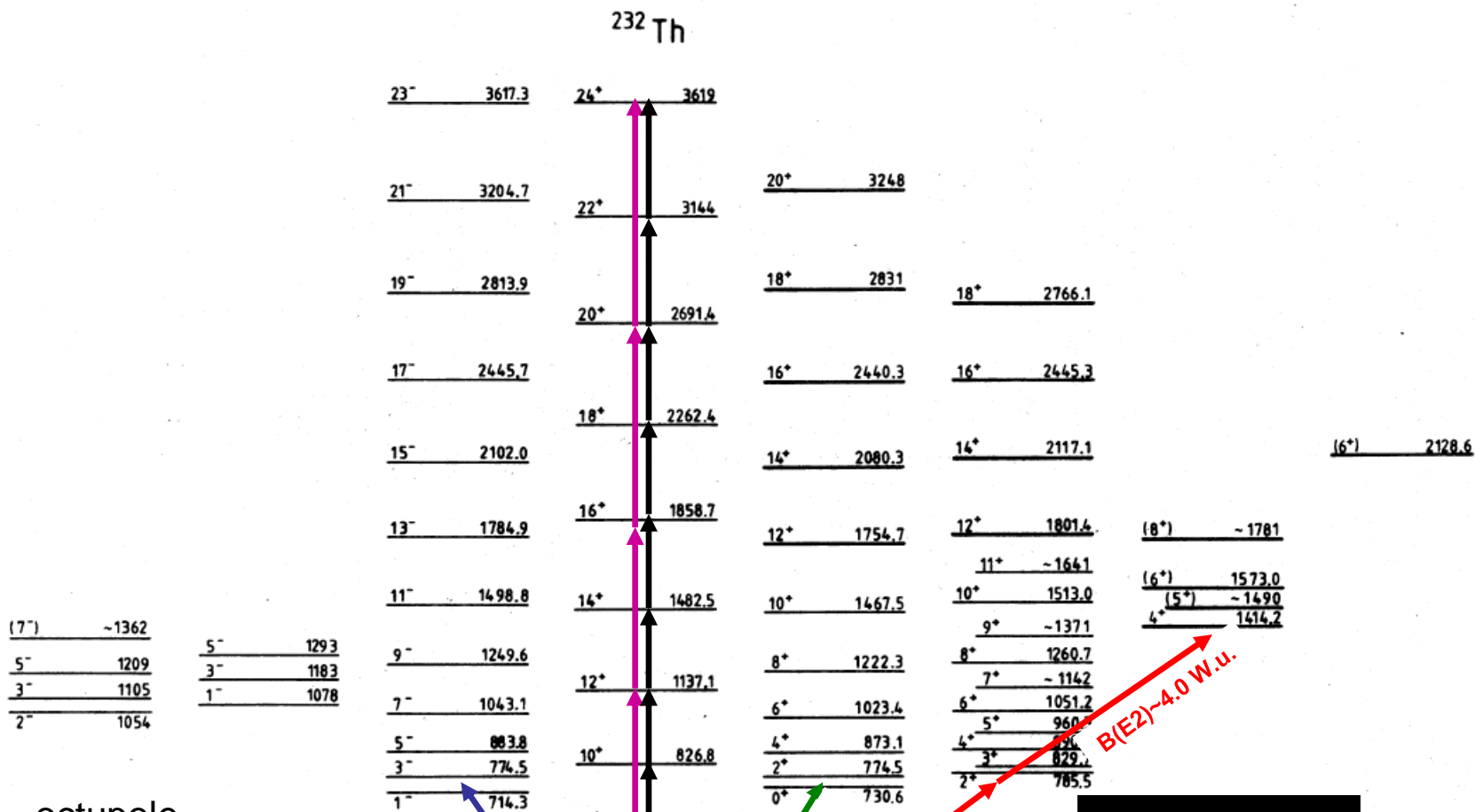


ex.: $^{90}\text{Zr} + ^{232}\text{Th}$ @ 396 MeV (4.44 MeV/u)
 backward angle scattering ($\theta > 100^\circ$)
 → favours multi-step excitation ($I \sim 20\hbar$)
 and higher lying states (β , γ , oct. vibration)

Excellent energy resolution (4keV@1MeV)
 but low Ge-Ge coincidence efficiency

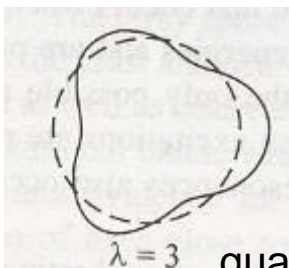
NaI-Ge coincidences and γ -ray multiplicity
 still allow to disentangle the level scheme

Multiple rotational band structure in ^{232}Th

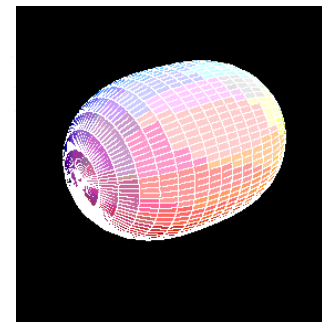
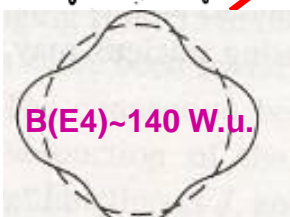


octupole

K^π :



quadrupole +
hexadecapole

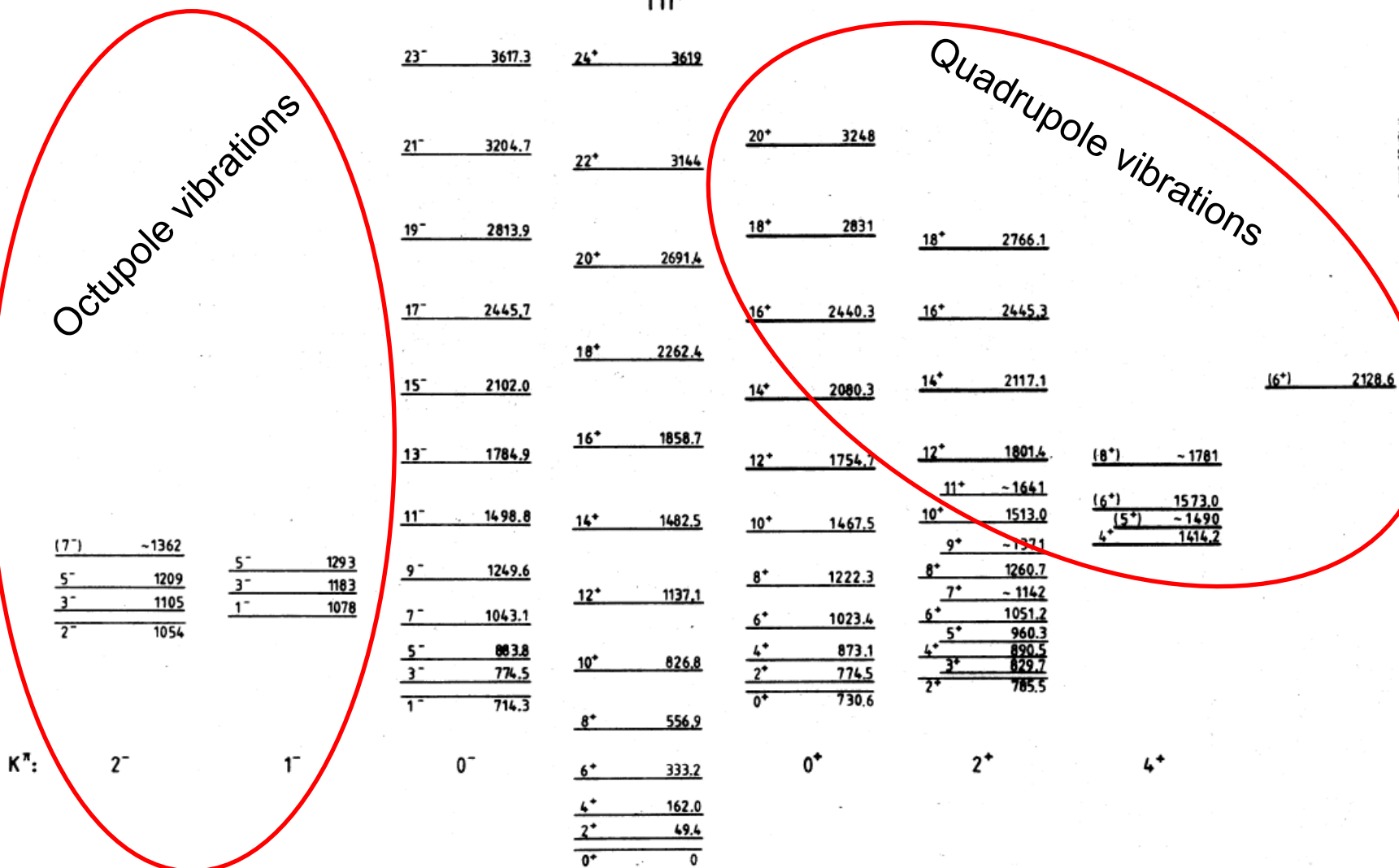


Multiple rotational band structure in ^{232}Th

^{232}Th

Octupole vibrations

Quadrupole vibrations



Multiple “vibrational” bands incl. inter-band $B(\sigma\lambda)$ and intra-band $B(E2)$ values (rotational model assumptions within the bands)

4π HPGe arrays with charged particle detectors

I r f u

cea

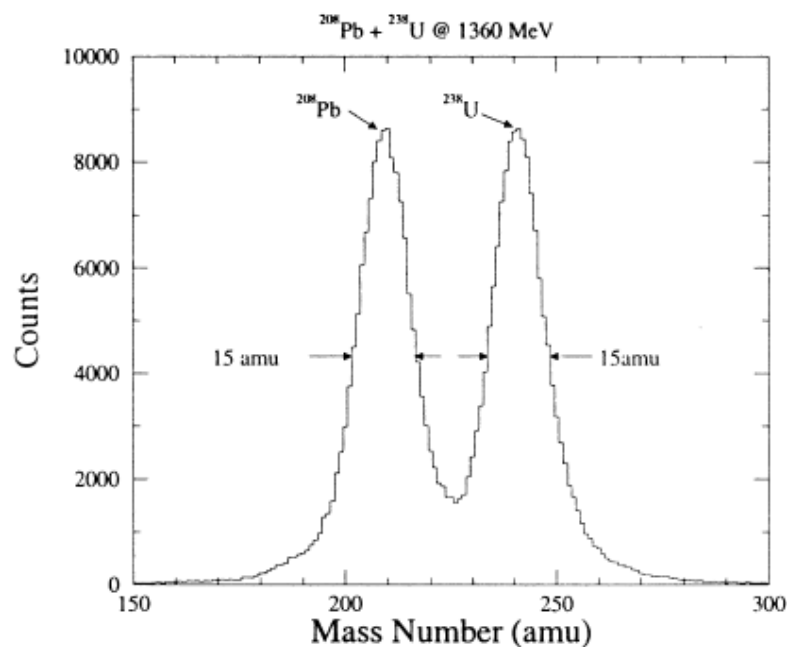
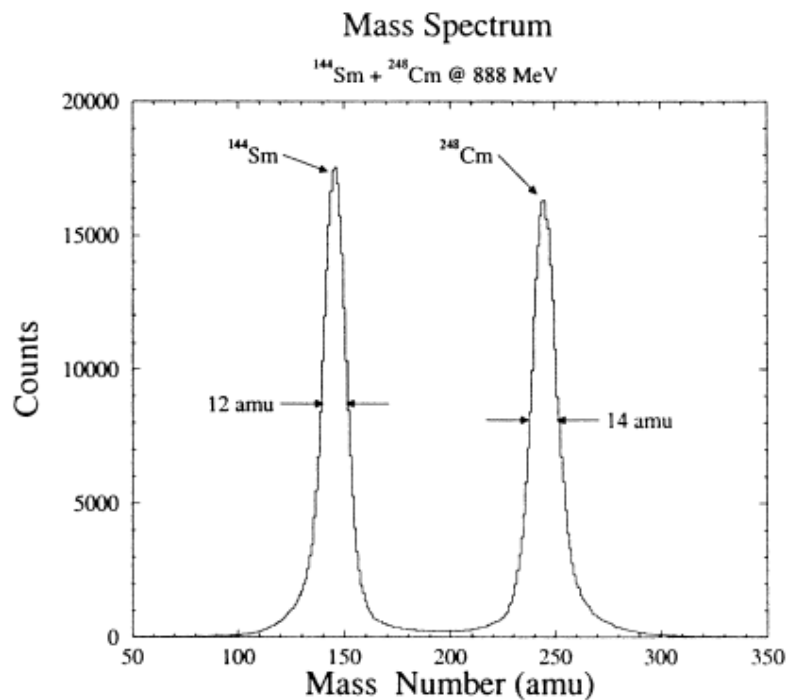
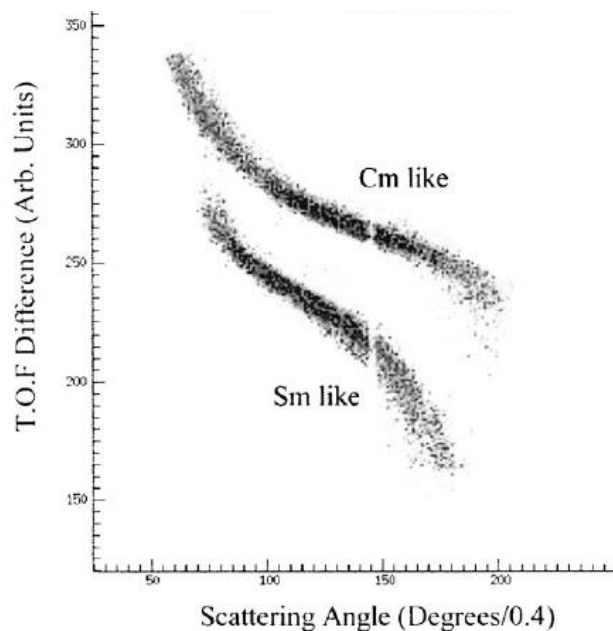
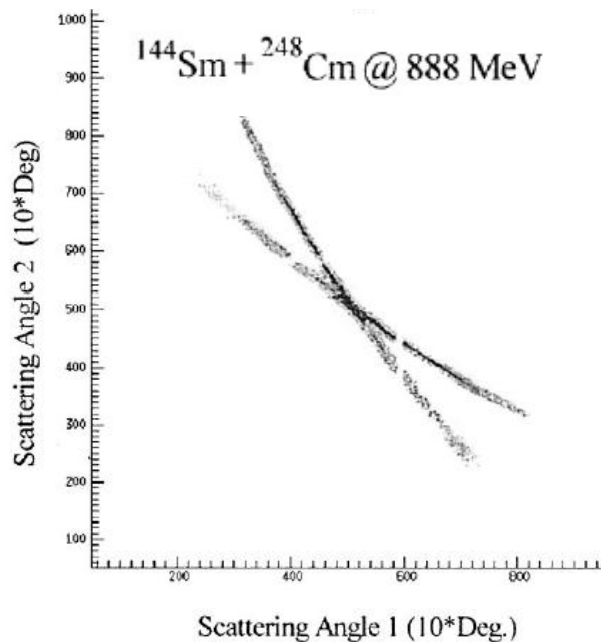
saclay

From ~1995: Ex. Chico 4π PPAC array (Univ. Rochester) and Gammasphere

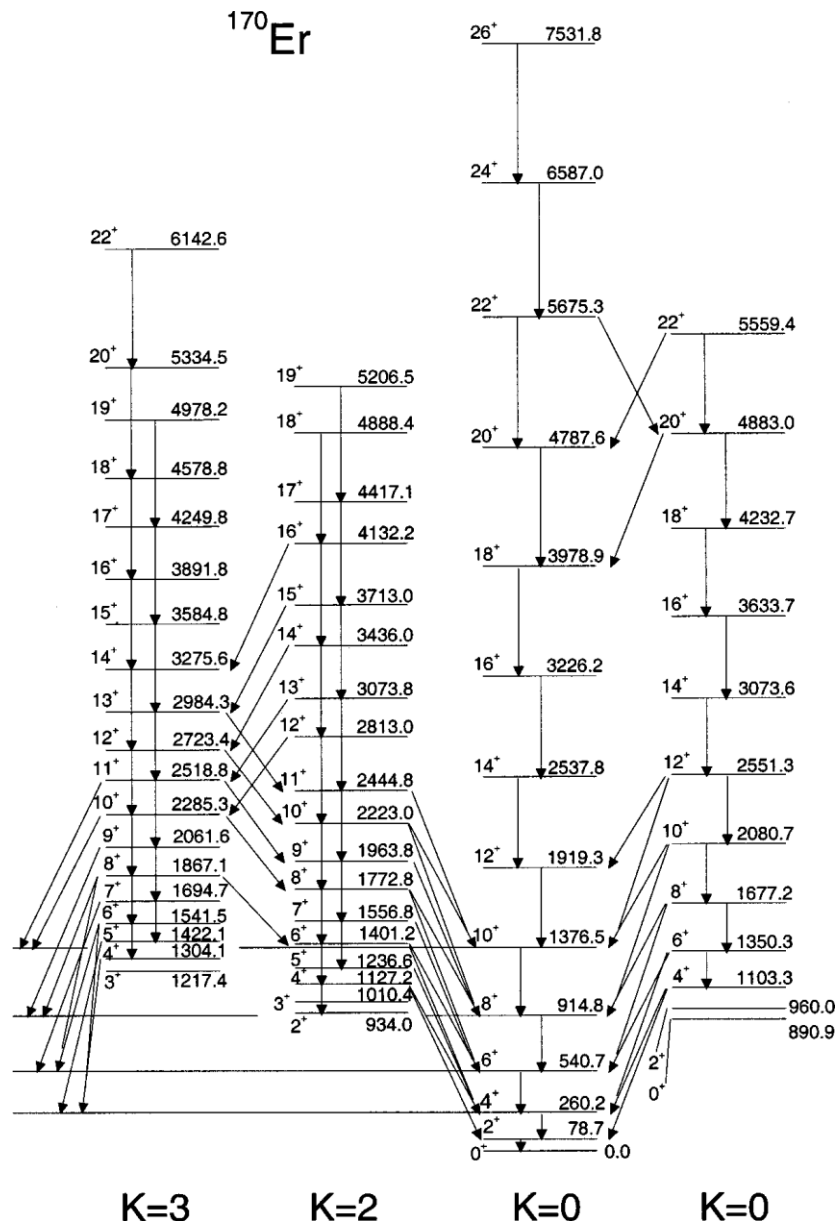
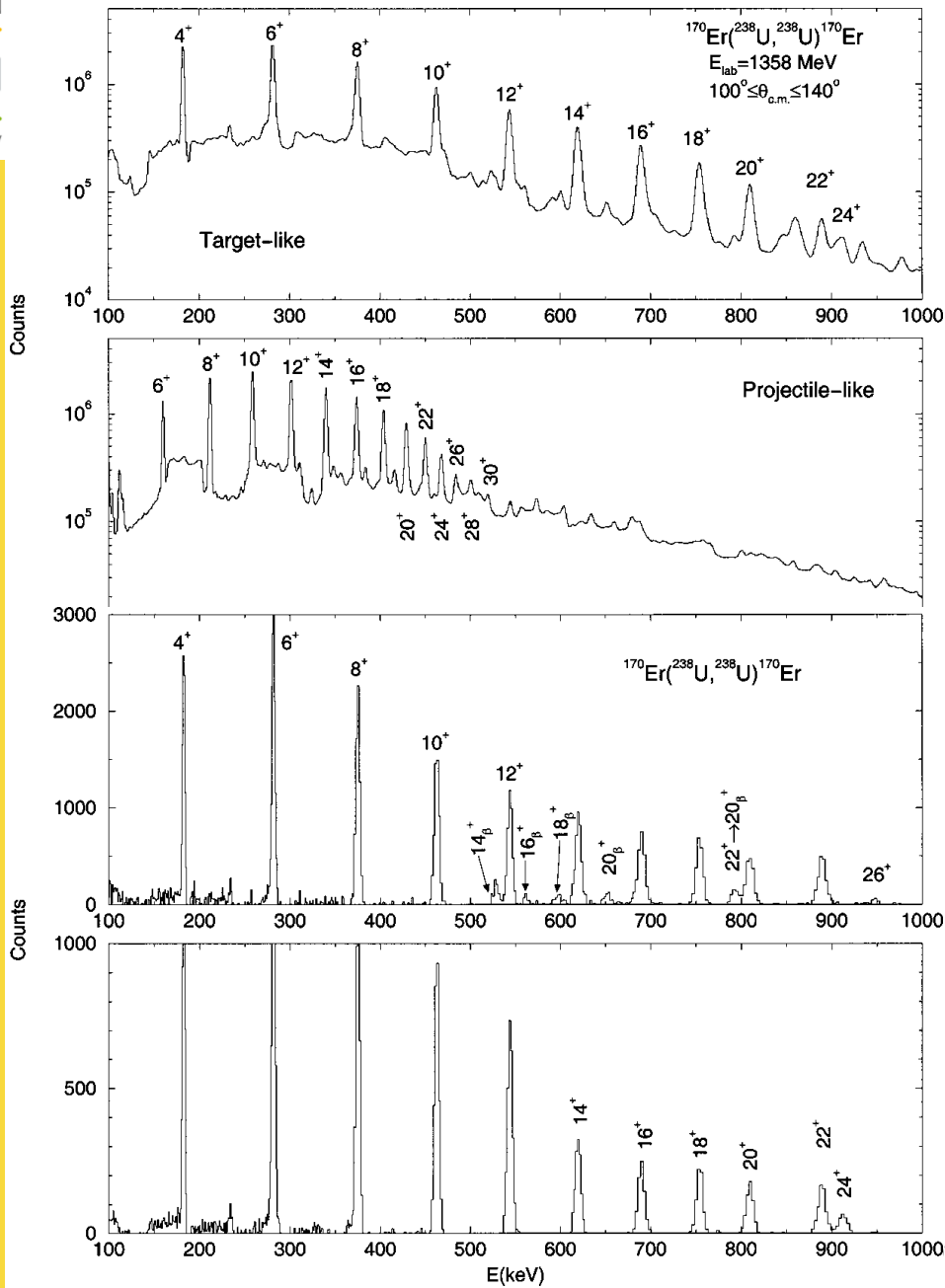


M.W.Simon, D. Cline, C.Y. Wu et al.,
Nucl. Inst. Meth. A452 (2000) 205

Performance of Chico PPAC



Some results from Chico and Gammasphere



Experimental results from Coulomb excitation

Need to deduce:

- **Velocity vectors of recoiling ions** (eventually also masses and reaction Q-value)
- **Correct for Doppler shift of de-excitation γ -rays** on an event-by-event basis
- **Identify γ -rays** which were emitted by each recoiling ion on an event-by-event basis
- **Normalize projectile yields** using an accurately known $B(E2)$: target or low-lying state
- **Determine Coulomb excitation cross sections** to excited states as function of impact parameter.
- **Use computer codes to extract individual electromagnetic matrix elements** from measured yields for both target and projectile excitation.

Expected results

- **Observation of (new) excited states**, in particular (higher lying) collective states (2_1^+ 4_1^+ 2_2^+ , ...)
- **$B(E2)$ and $B(M1)$ values** between (all) low-lying states, eventually also higher $B(E\lambda)$ values
- **Sign and magnitude of static E2 moments** of excited states
- **Signs and magnitudes of observable products of $E\lambda$ matrix elements**
- **M1 moments of excited states** may be obtained from the measured **attenuation of the γ -ray angular correlations** for ions recoiling in vacuum

Rochester - Warsaw GOSIA computer code

l r f u

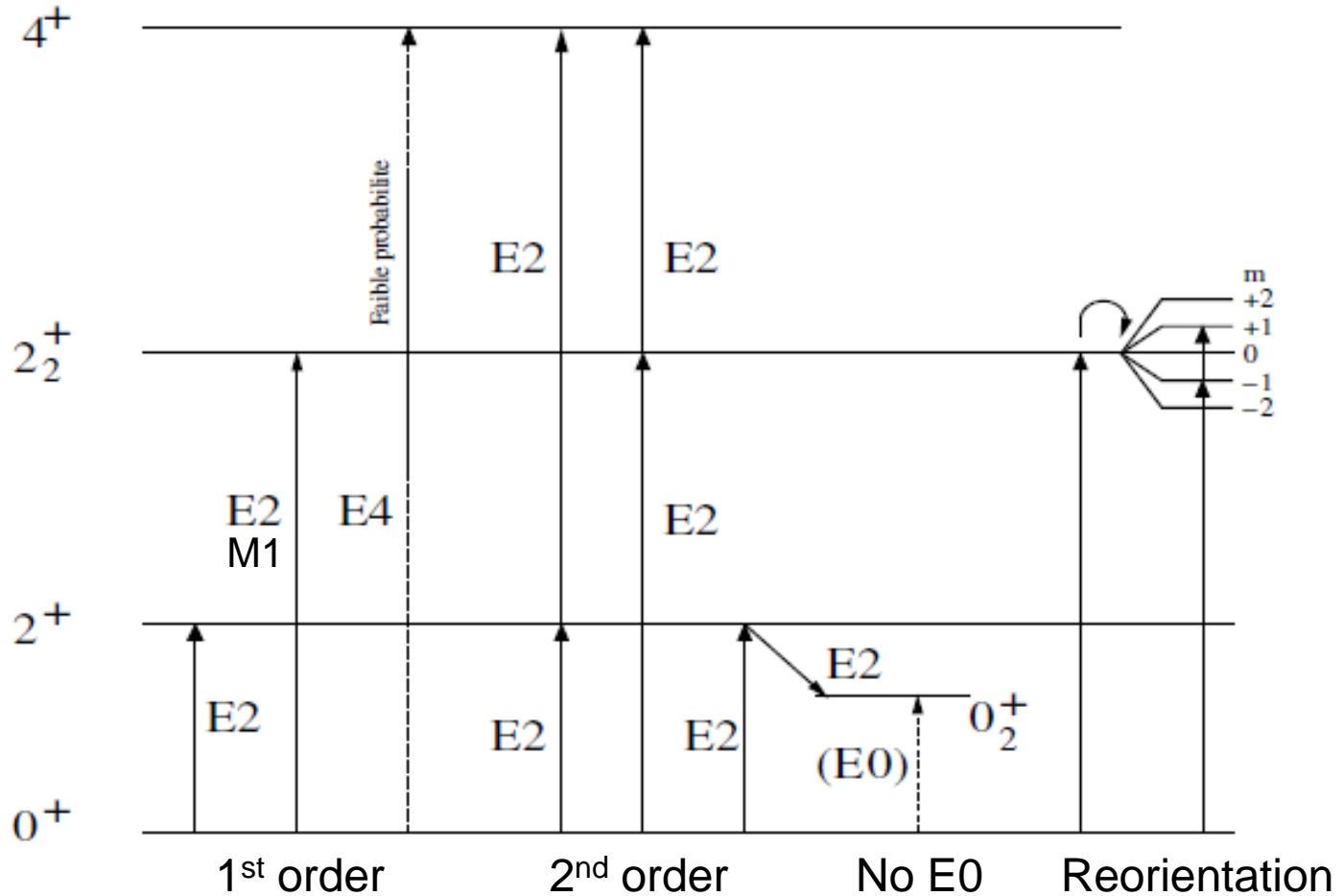
cea

saclay

I) Excitation stage:

- 1) Semi-classical approximation and pure electromagnetic interaction
 - max. 5% deviation from full quantal calculation at $\eta \sim 30$
- 2) Classical hyperbolic trajectories
 - symmetrised in energy : $v_{\infty} \rightarrow \frac{1}{2}(v_i + v_f)$
 - atomic screening, vacuum polarization, relativistic effects ignored
 - ➔ change in distance of closest approach $< 0.2\%$
- 3) Virtual excitation of unobserved states
 - Include higher lying (unobserved) states
 - Include Giant E1 Resonance through dipole polarisation term (12%)
- 4) Mutual excitation of colliding nuclei
 - Monopole-multipole interaction of either the target or projectile
 - ➔ multipole-multipole correction very small (0.05% in mass-70)
 - Mutual excitation explicitly treated in new code (Gosia2)
- 5) Particle solid angle and target thickness
 - Numerical integration over solid angle of particle detectors and energy loss in the target
 - ➔ excitation probability and statistical tensor for ALL excited states

Model for GOSIA excitation stage



Rochester - Warsaw GOSIA computer code

l r f u

cea

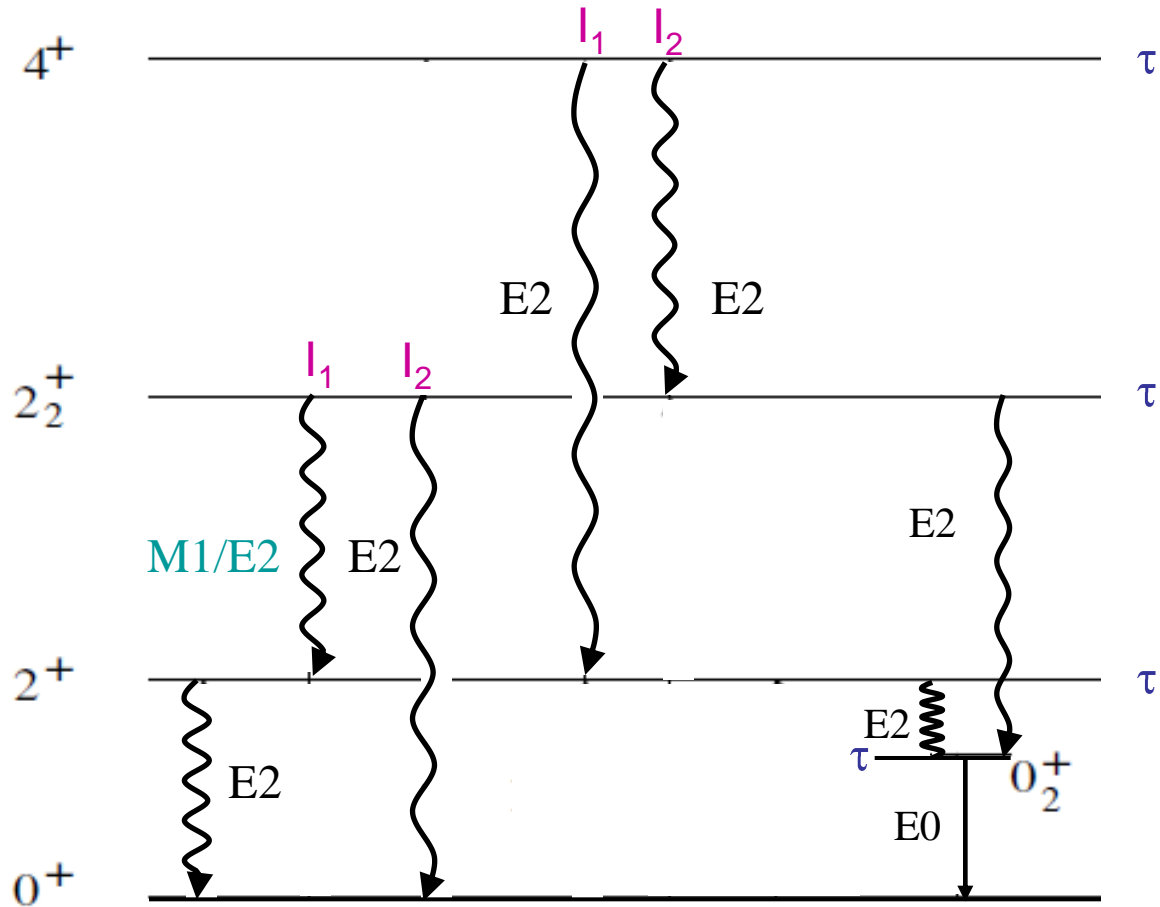
saclay

II) Decay stage:

- 1) Use **statistical tensors** calculated in the excitation stage
 - Information on excitation probability and initial sub-state population
- 2) Include **cascade feeding** from higher-lying states
- 3) Include **deorientation of the angular distribution** (due to recoil in vacuum)
 - two-state model by Brenn and Spehl to model hyperfine interactions
- 4) Include **Relativistic transformation** of solid angles
- 5) Include **solid angle of gamma-ray detectors**
 - Simplified (cylindrical) detector geometry with attenuation factors
- 6) Possibility to include in-flight decays for long-lived states

➔ calculate gamma ray yields for all possible transitions

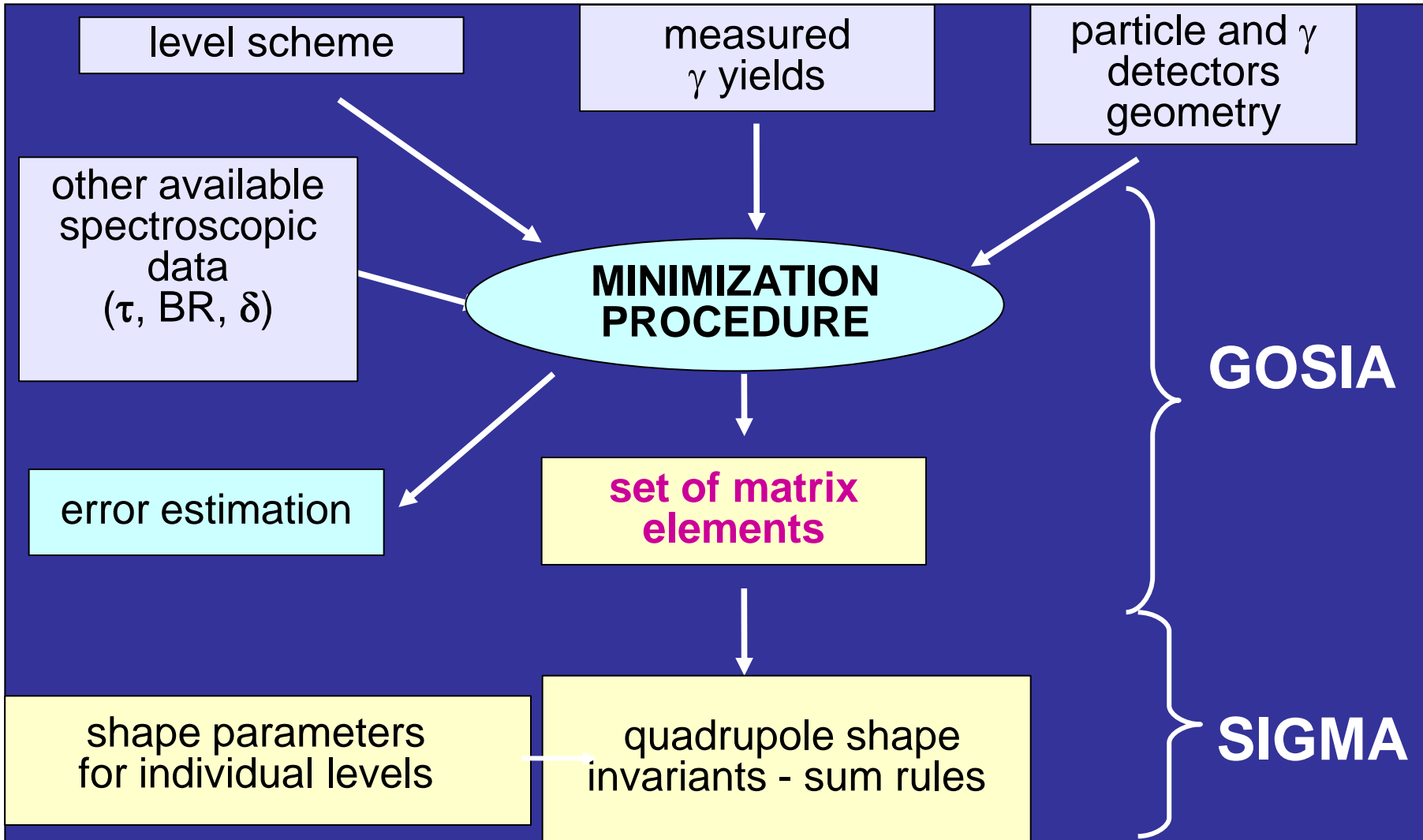
Model for GOSIA decay stage



Lifetimes, branching and mixing ratios from independent sources can be added as additional constraints

Rochester - Warsaw GOSIA computer code

GOSIA is a semi-classical coupled-channel Coulomb excitation code using a two-stage approach and a least-squares search to reproduce experimentally observed gamma-ray intensities



Coulomb excitation studies using radioactive beams

Production and reacceleration schemes for ISOL beams at different facilities

I r f u

cea

saclay

GANIL/SPIRAL: Heavy Ion beam (50-100 MeV/u) & Cyclotron (3-20 MeV/u)

ISOLDE/REX: Proton beam (1.4 GeV, $3 \cdot 10^{13}$ /pulse) & HI Linac (3 MeV/u)

TRIUMF/ISAC: Proton beam (500 MeV, 0.1 mA) & HI Linac (2/5 MeV/u)

ORNL/HRIBF: Low-energy proton induced fission & Tandem (2-5 MeV/u)

Principal differences in

production	→ fragmentation, spallation, fission
preparation	→ extraction, selection, ionisation
availability	→ elements & mass range, purity
acceleration	→ beam energy & possible reactions

“Ideal” ISOL facility does not yet exist, soon **SPIRAL2**, **HIE-ISOLDE**, **ISAC2**
Highest yields over largest part of the nuclear chart (not only fission fragm.)
Largest variety and best purity of beams with well-defined beam energy

Experimental considerations for RIB experiments

l r f u

cea

saclay

Principle

- Scattering of a (radioactive) ion beam on a (high-Z) target at “safe” energy
- Choice of target depends (mainly) on available beam energy and state(s) of interest

Experimental Method:

- Use **thin targets** so that excited nuclei (and the unscattered beam) recoil in vacuum
- Measure **scattering angles and velocities of recoiling ions** over a wide range of scattering angles
- Detect deexcitation **γ -rays in coincidence with the scattered ions**

Principal difficulties

- Background from radioactive decay of beam particles (Rutherford)
- Beam contaminants (isobars)
- Low beam intensity and limited statistics (in particular of higher lying states)

Coulomb excitation set up with radioactive ions

- Identification of reaction partners
 - Energy deposition in Si detector

- Differential cross section
 - annular rings
 - projectile and recoil detection
 - ➔ $30^\circ < \theta_{CM} < 130^\circ$

- Identification of excited states

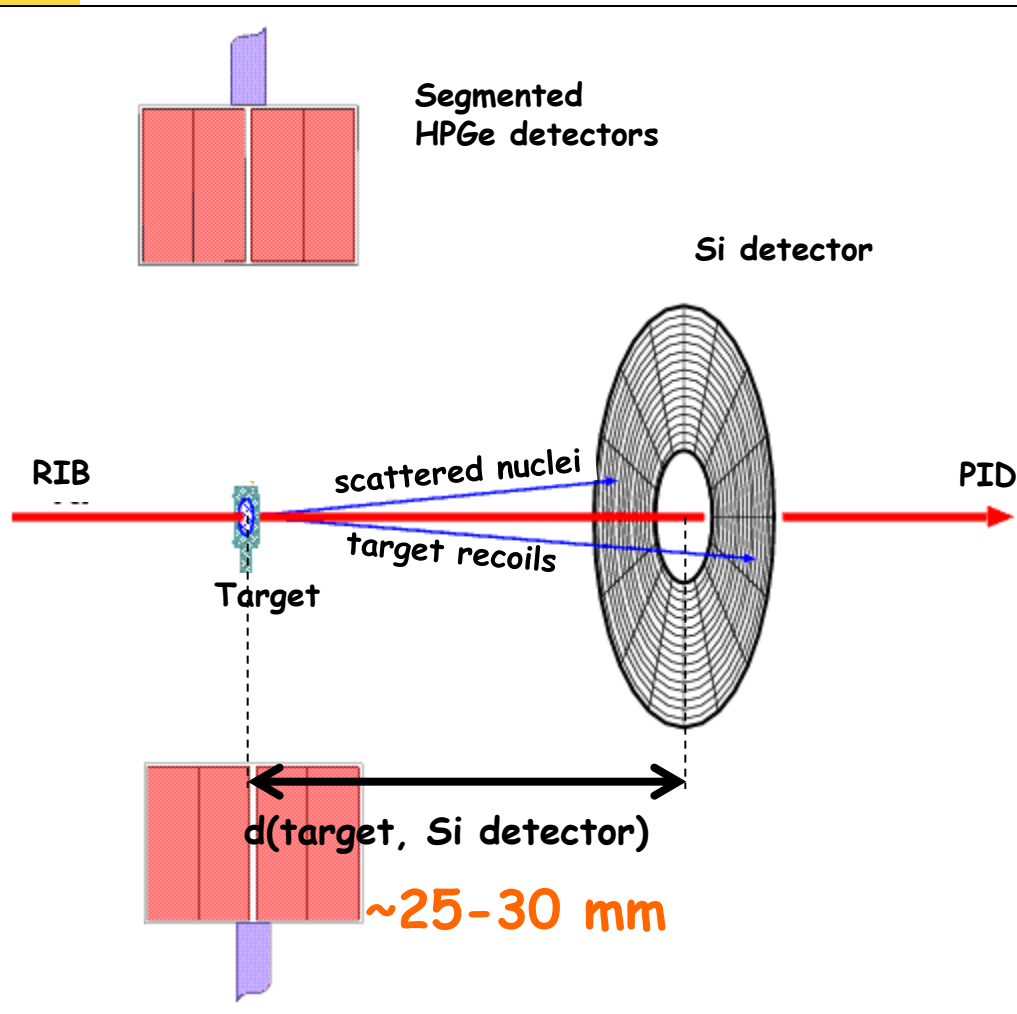
- Large volume Ge detectors
 - ➔ high resolution gamma-ray spectroscopy (few keV)

- Doppler correction ($v/c \sim 10\%$)

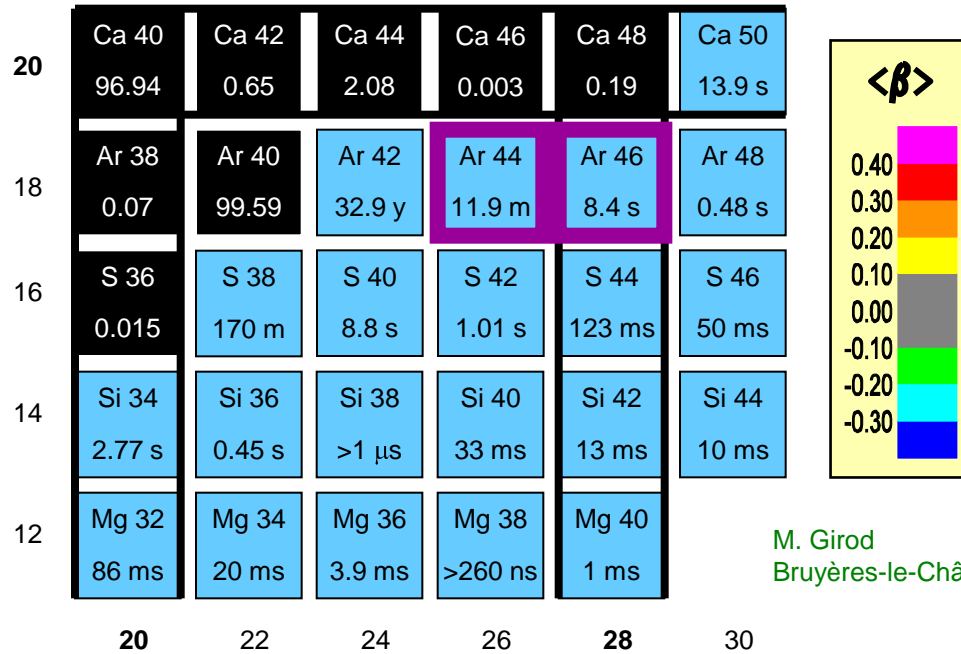
- highly segmented Si detector
- highly segmented Ge detectors

- Trigger condition

- Ge-Si coincidences:
 - differential cross section, gamma background reduction
- Si singles data: normalisation



Shape coexistence in N=28 isotones



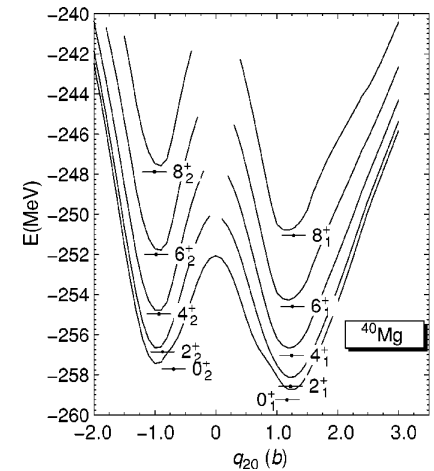
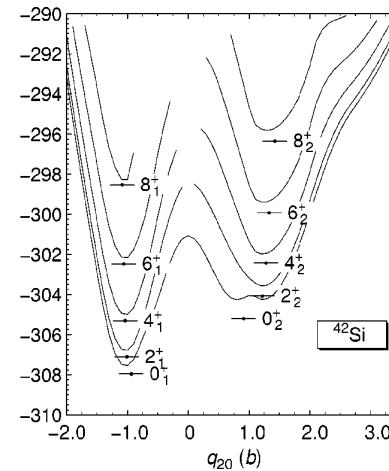
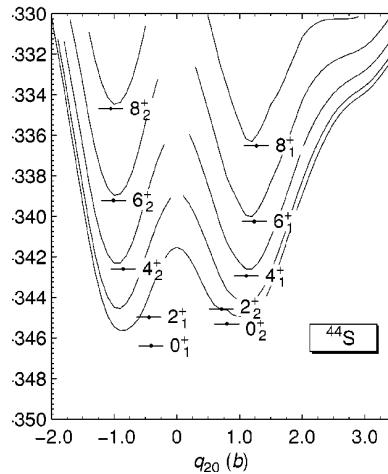
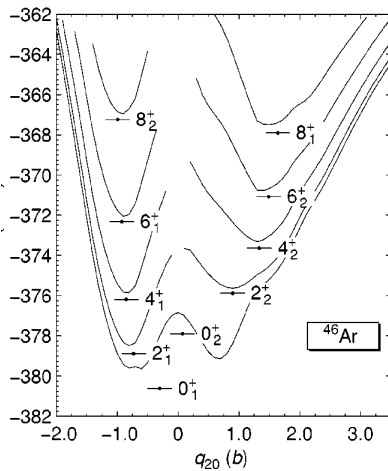
Rapid onset of deformation in N~28 nuclei below Ca ?

All N=28 isotones predicted to show shape coexistence

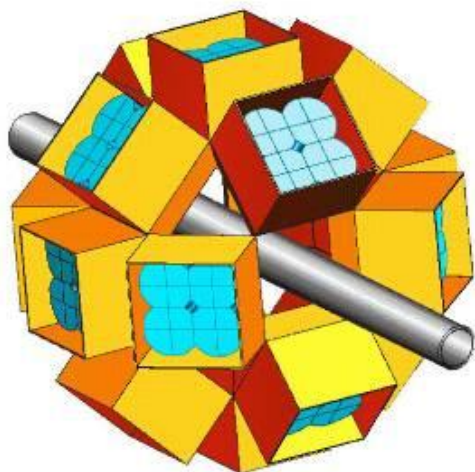
Precision measurement of e.m. matrix elements in ^{44}Ar

M. Girod
Bruyères-le-Châtel

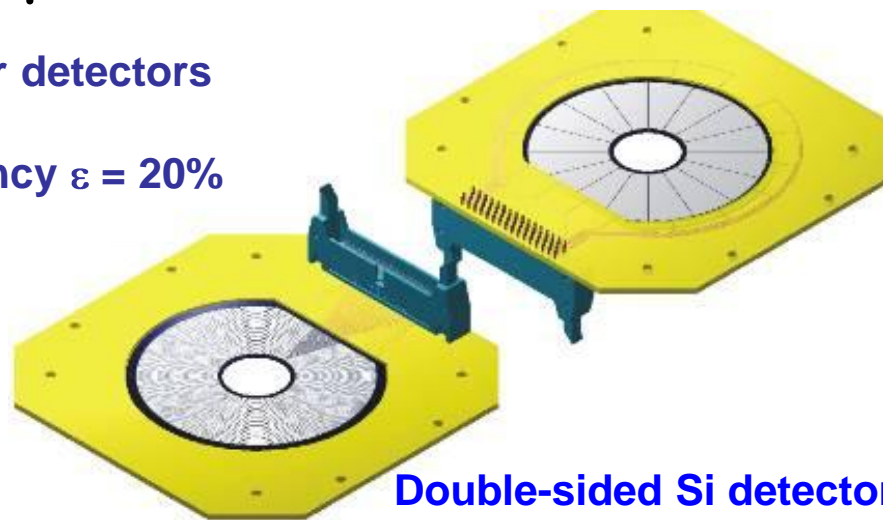
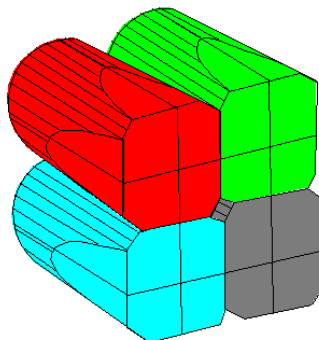
R. Rodríguez-Guzmán, PRC 65, 024304



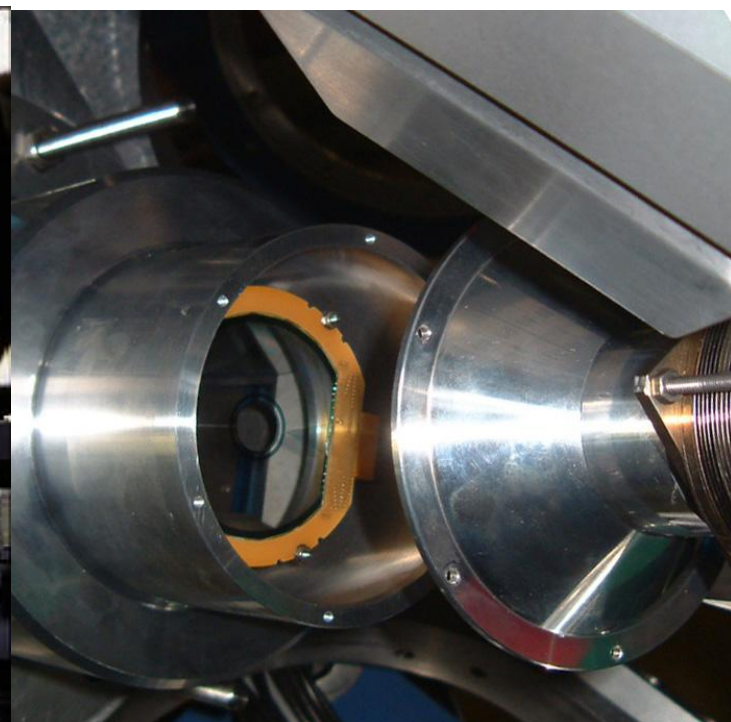
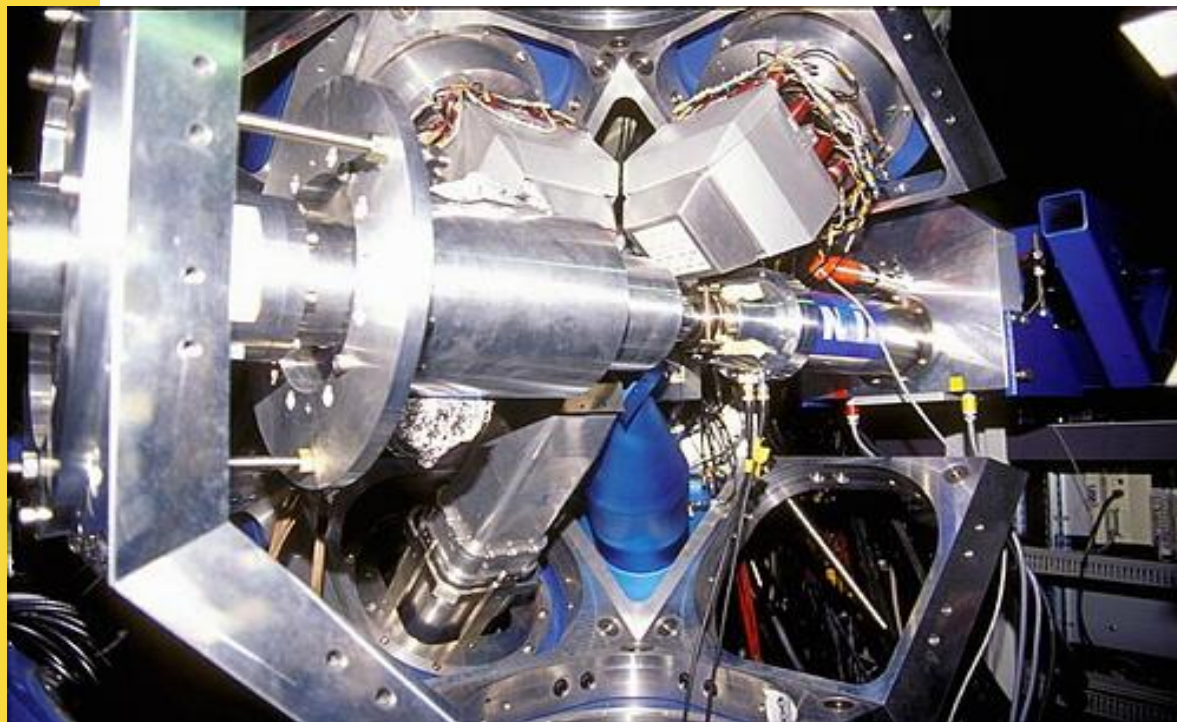
Coulomb excitation set-up for RIBs (ex. SPIRAL)



16 large Ge Clover detectors
4 × 4 segmented
photopeak efficiency $\varepsilon = 20\%$

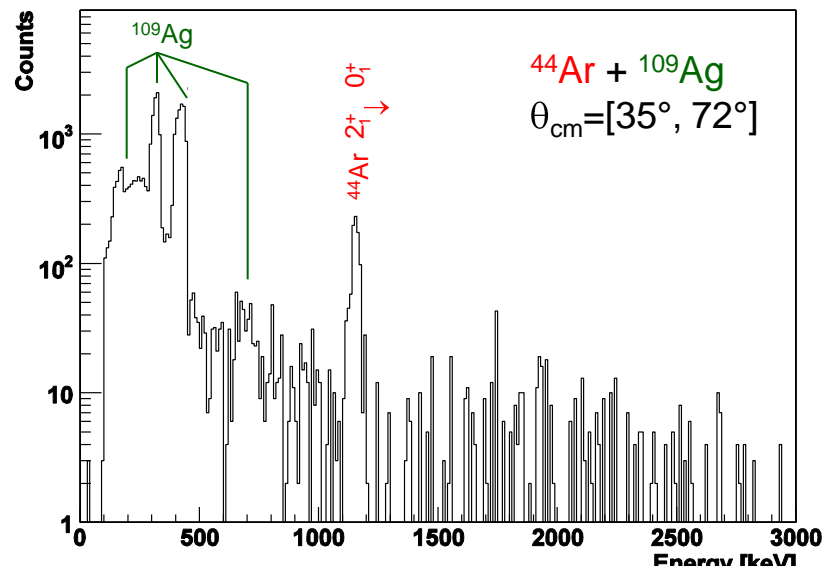
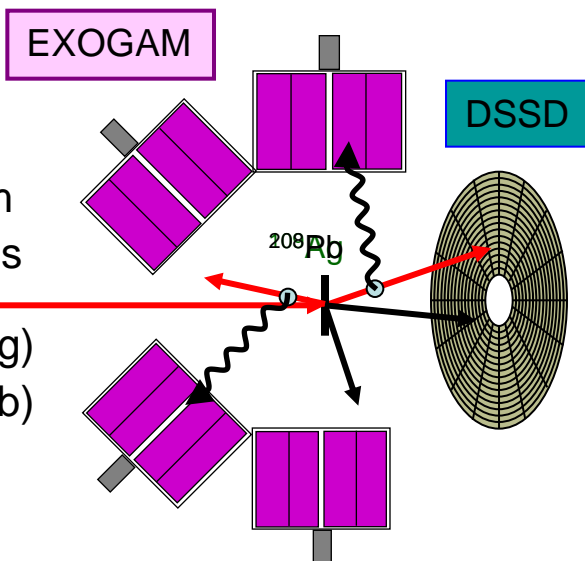


Double-sided Si detector
48 rings × 16 sectors

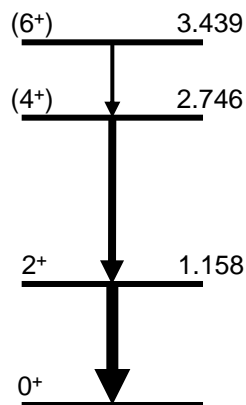


Coulomb excitation of ^{44}Ar at SPIRAL / GANIL

SPIRAL beam
 ^{44}Ar $3 \cdot 10^5$ pps
 2.8-A MeV (Ag)
 3.8-A MeV (Pb)

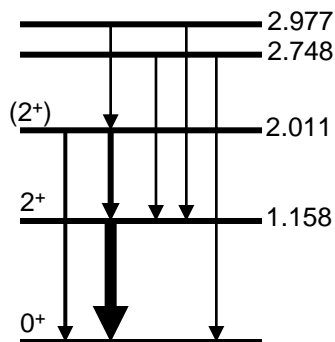


deep inelastic

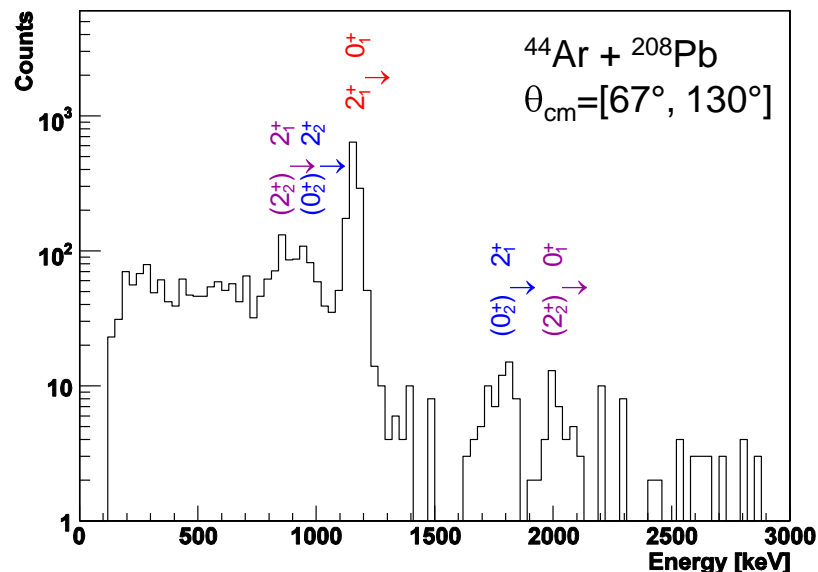


B. Fornal et al.,
 EPJA 7, 147 (2000)

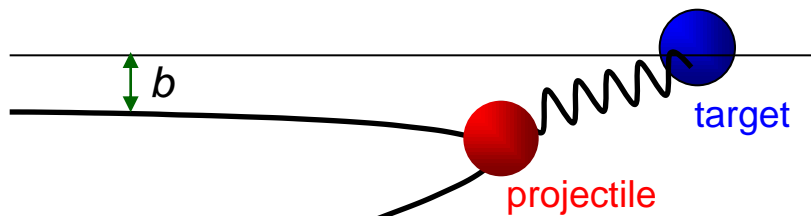
beta decay



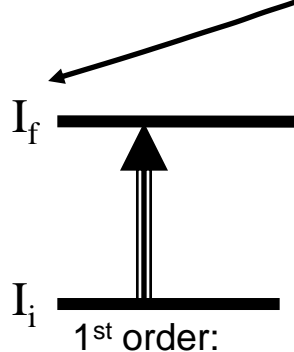
J. Mrazek et al.,
 Nucl. Phys. A 734, E65 (2004)



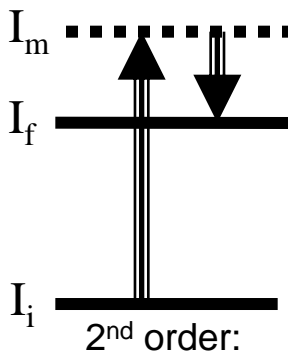
Determination of quadrupole moments



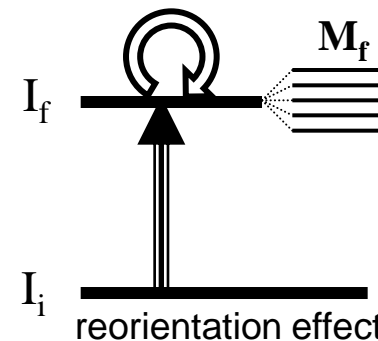
The excitation cross section is a direct measure of the $E\lambda$ matrix elements.



$$a_{i \rightarrow f}^{(1)} \propto \langle I_f \| \mathbf{M}(E2) \| I_i \rangle$$



$$a_{i \rightarrow f}^{(2)} \propto \langle I_f \| \mathbf{M}(E2) \| I_m \rangle \langle I_m \| \mathbf{M}(E2) \| I_i \rangle$$



$$a_{i \rightarrow f}^{(2)} \propto \langle I_f \| \mathbf{M}(E2) \| I_f \rangle \langle I_f \| \mathbf{M}(E2) \| I_i \rangle$$

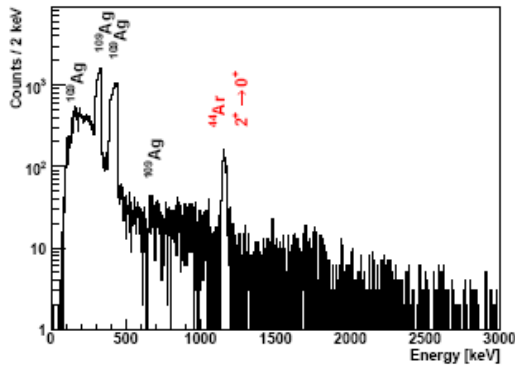
$$P_{0 \rightarrow 2}^{(2)}(\mathcal{G}, \xi) = P_{0 \rightarrow 2}^{(11)}(\mathcal{G}, \xi) \left[+ q \cdot K(\mathcal{G}, \xi) \right]$$

$$q = \frac{A_{T/P} \Delta E_{MeV}}{Z_{P/T} (1 + A_P / A_T)} \sqrt{\frac{7}{2\pi}} \frac{5}{4} Q_2$$

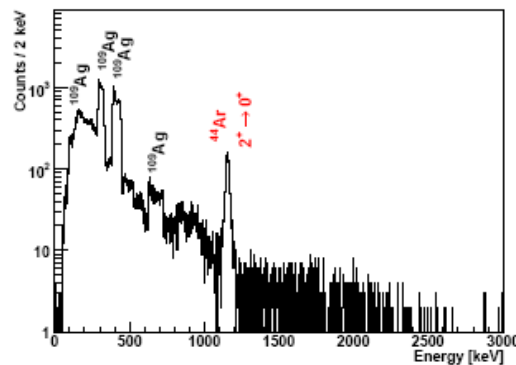
Sensitivity to Q_2 by varying Z , θ , $\xi(a, v_\infty)$

Coulomb excitation of ^{44}Ar at SPIRAL / GANIL

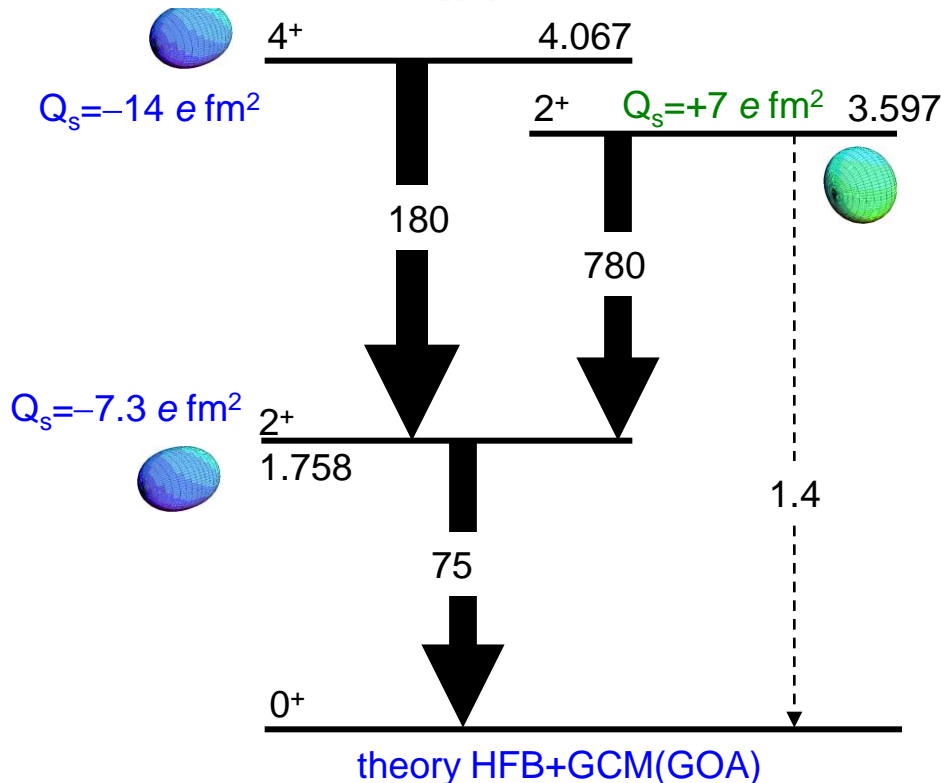
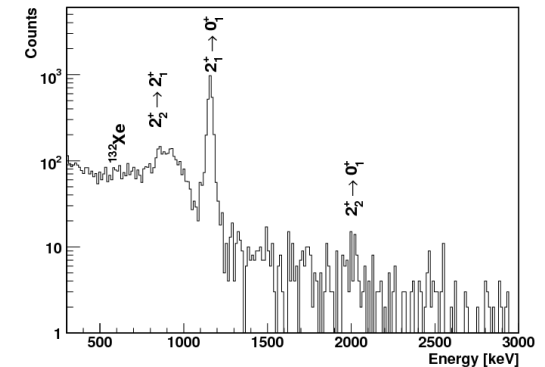
Ag target, $35^\circ < \theta_{\text{cm}} < 70^\circ$



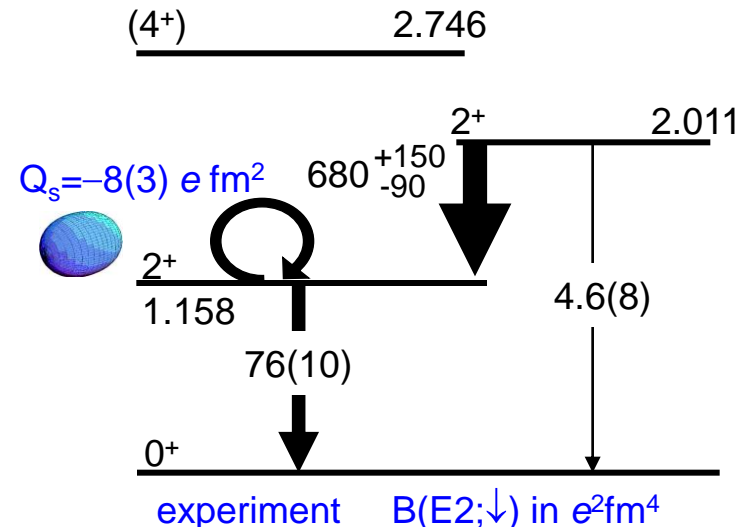
Ag target, $70^\circ < \theta_{\text{cm}} < 130^\circ$



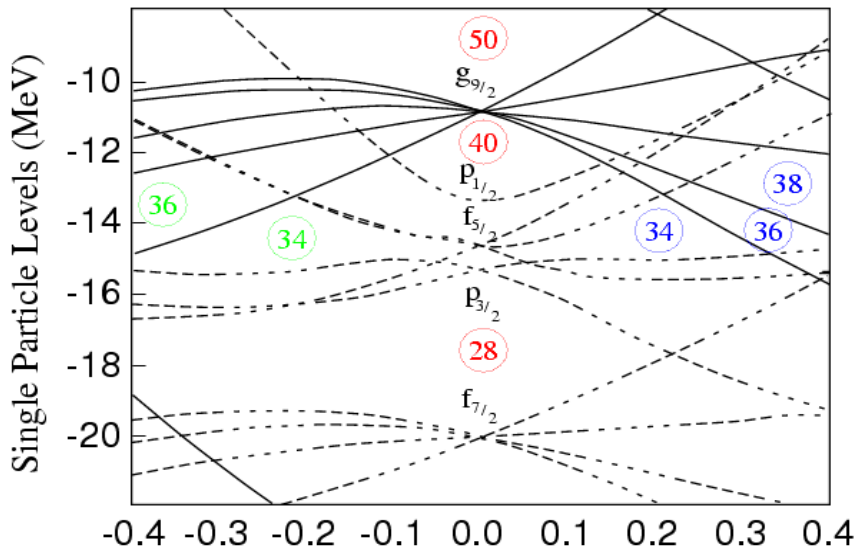
Pb target, $30^\circ < \theta_{\text{cm}} < 130^\circ$



- good agreement for $B(E2)$ and Q
- energy spectrum too spread out



Shape coexistence around A=70



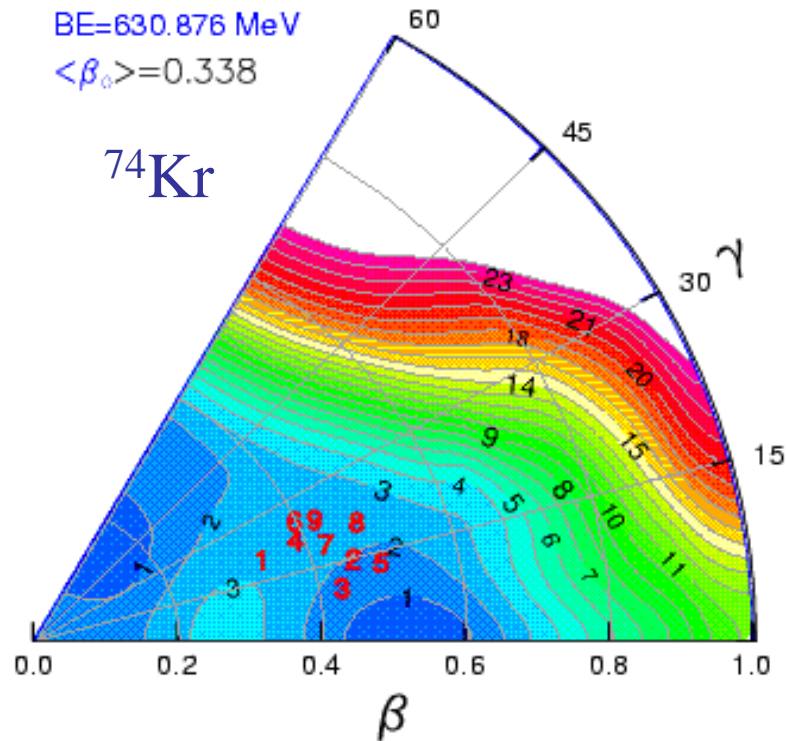
expected e.g. in:



BE=630.876 MeV

$\langle \beta_0 \rangle = 0.338$

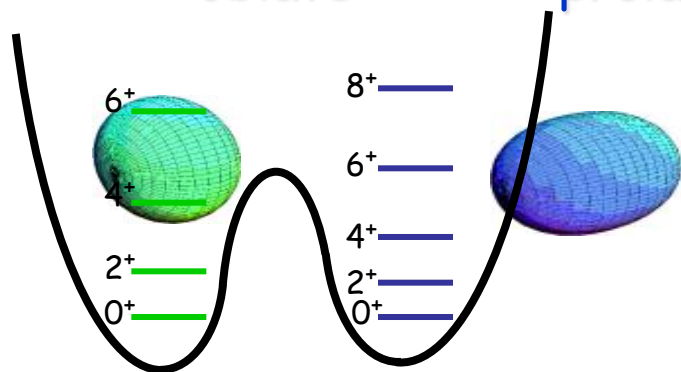
${}^{74}\text{Kr}$



oblate

β

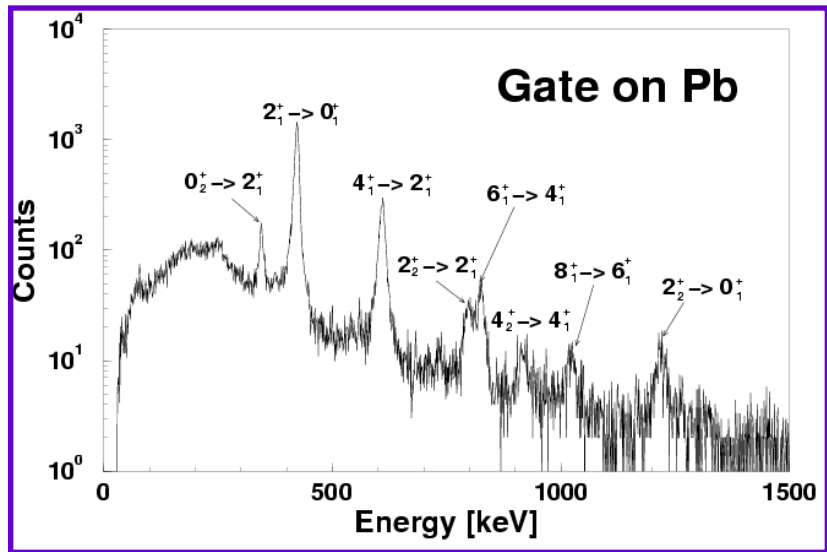
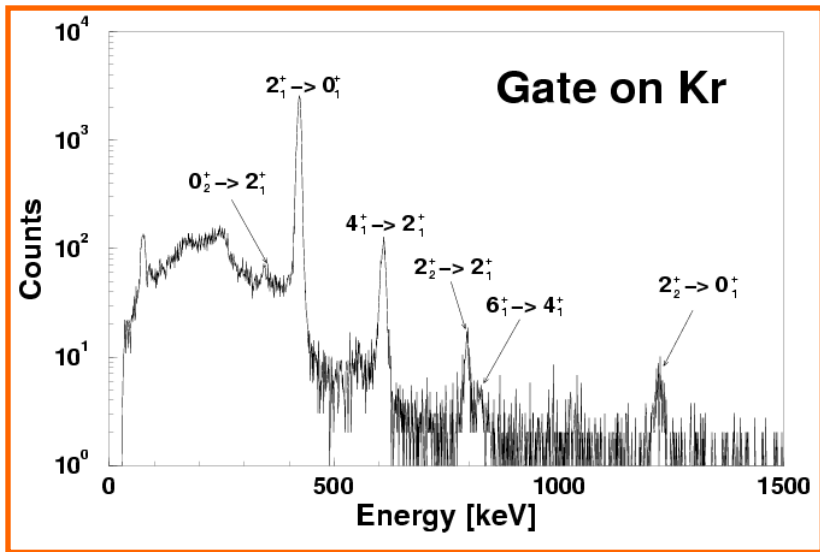
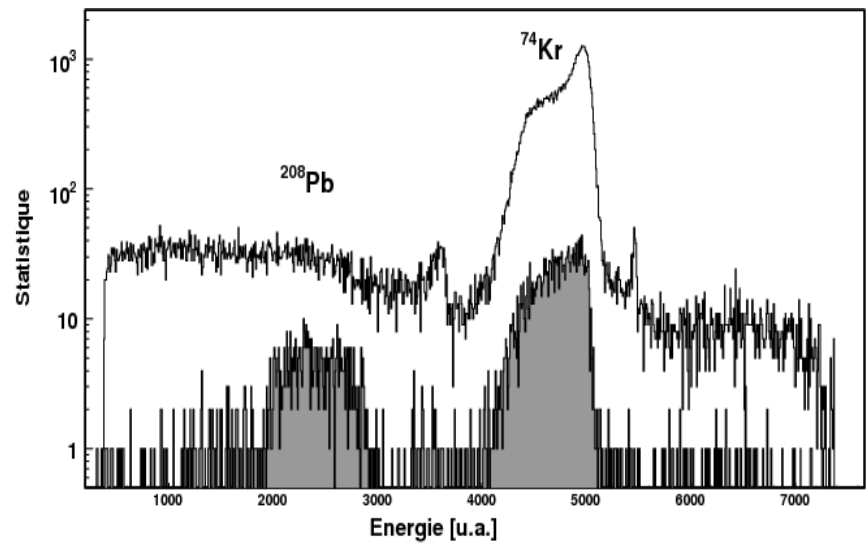
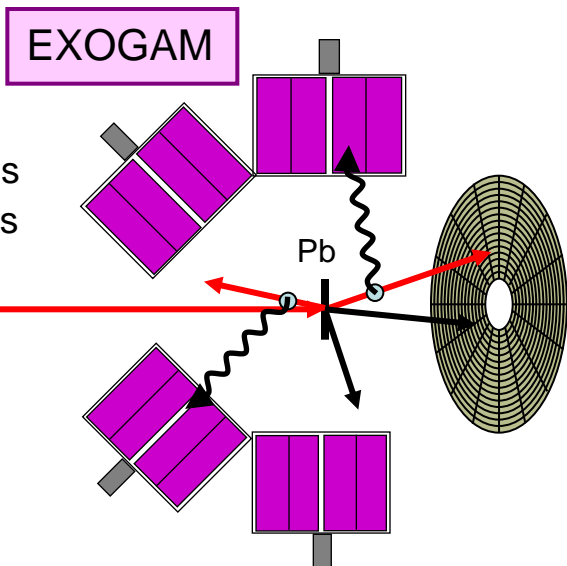
prolate



Possible 0^+ shape isomers and configuration mixing

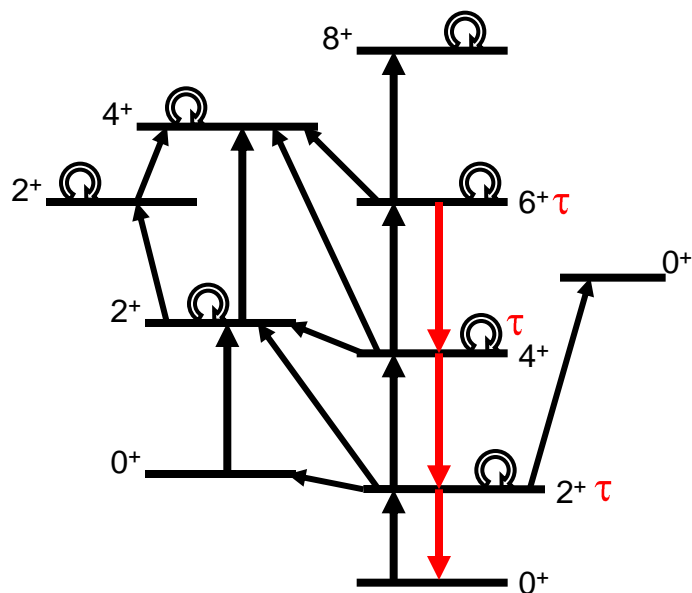
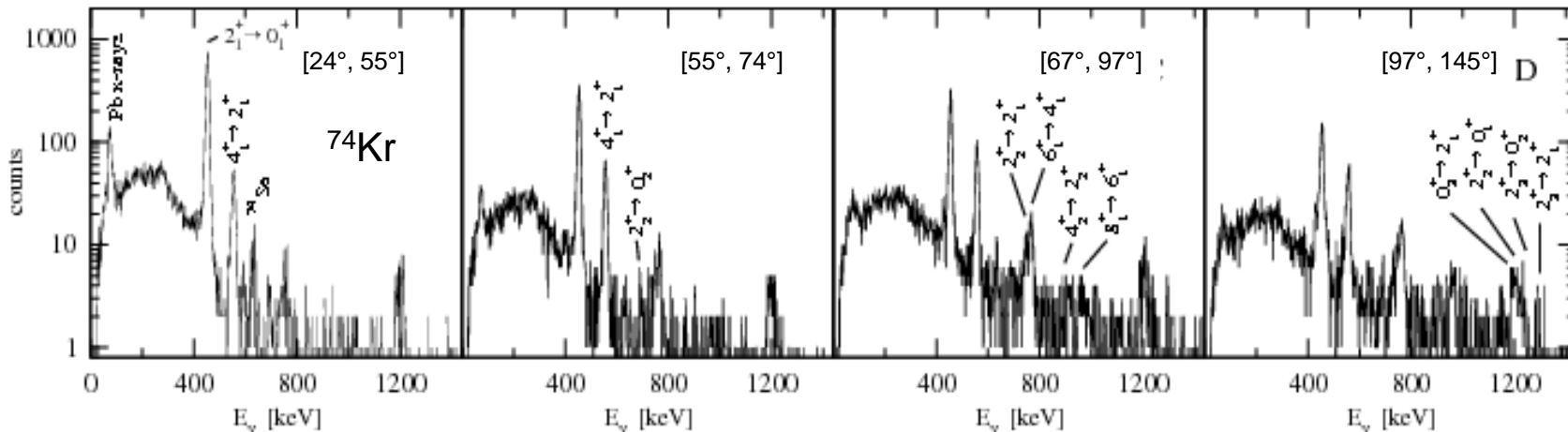
Coulomb excitation of $^{74,76}\text{Kr}$ at SPIRAL

SPIRAL beams
 ^{76}Kr 5×10^5 pps
 ^{74}Kr 10^4 pps
 4.5 MeV/u



Acta Phys. Pol. B 36, 1281 (2005)

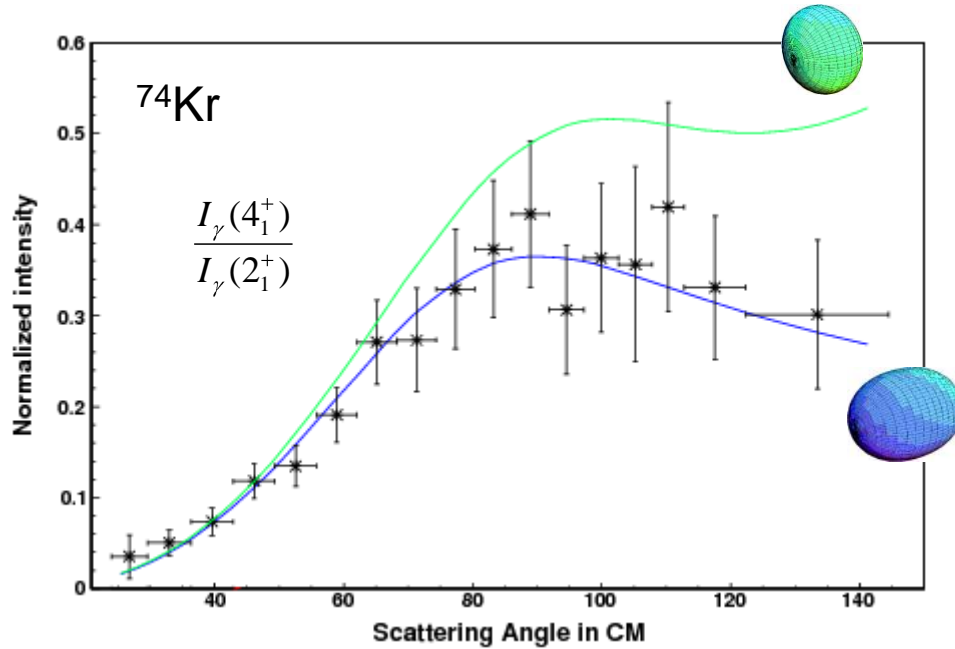
Shape coexistence in ^{74}Kr



- $^{74}\text{Kr} + ^{208}\text{Pb}$ at 4.7 MeV/u (SPIRAL)
 - ➔ multi-step Coulomb excitation
- γ -ray yields as function of scattering angle (differential excitation cross section)
- experimental spectroscopic data (lifetimes, branching ratios)
- least squares fit of ~ 30 matrix elements (transitional and diagonal)

E. Clément et al., Phys. Rev. C 75, 054313 (2007)

Sensitivity to quadrupole moments



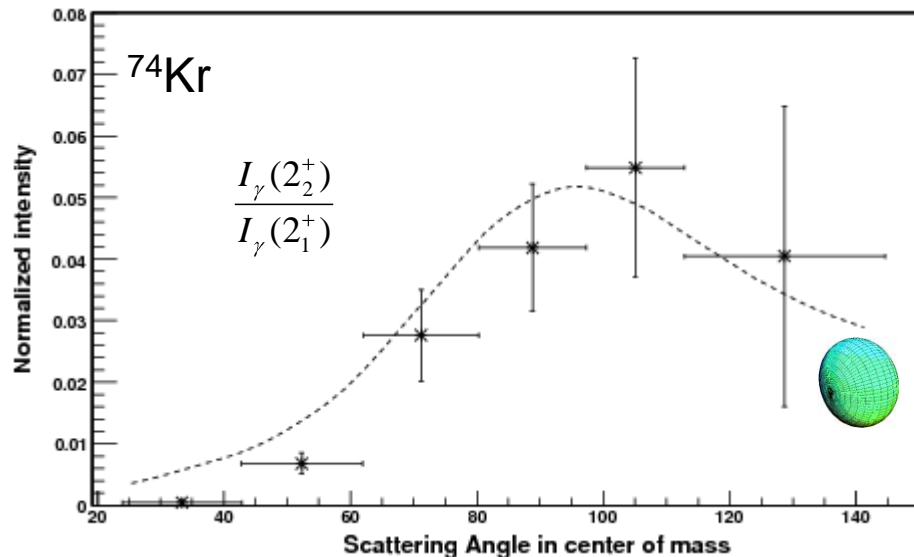
full χ^2 minimization:

$$\langle 2_1^+ \| \mathbf{M}(E2) \| 2_1^+ \rangle = -0.70_{-0.30}^{+0.33}$$

$$\langle 4_1^+ \| \mathbf{M}(E2) \| 4_1^+ \rangle = -1.02_{-0.21}^{+0.59}$$

negative matrix element
(positive quadrupole moment Q_0)

\Rightarrow prolate shape

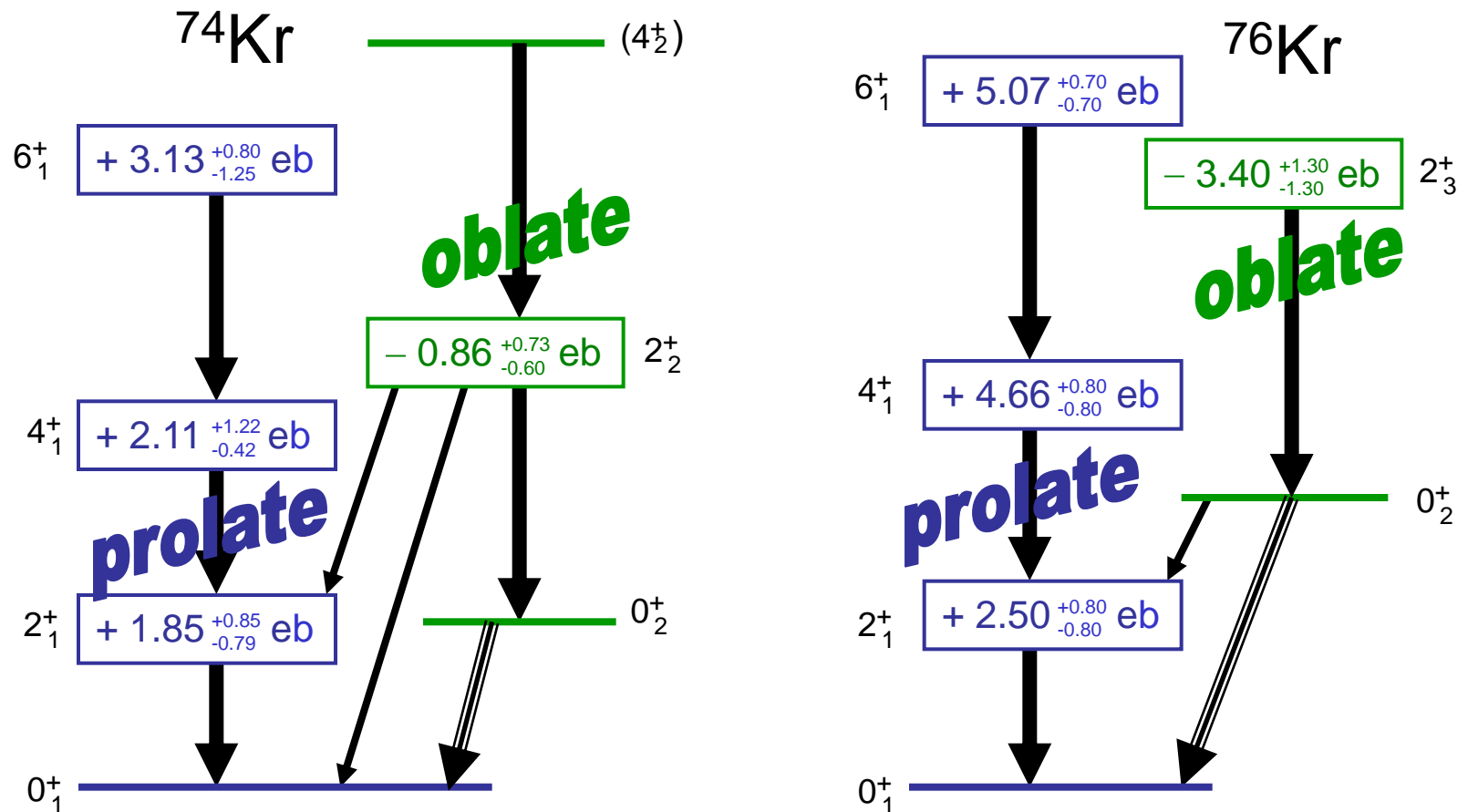


$$\langle 2_2^+ \| \mathbf{M}(E2) \| 2_2^+ \rangle = +0.33_{-0.23}^{+0.28}$$

positive matrix element
(negative quadrupole moment Q_0)

\Rightarrow oblate shape

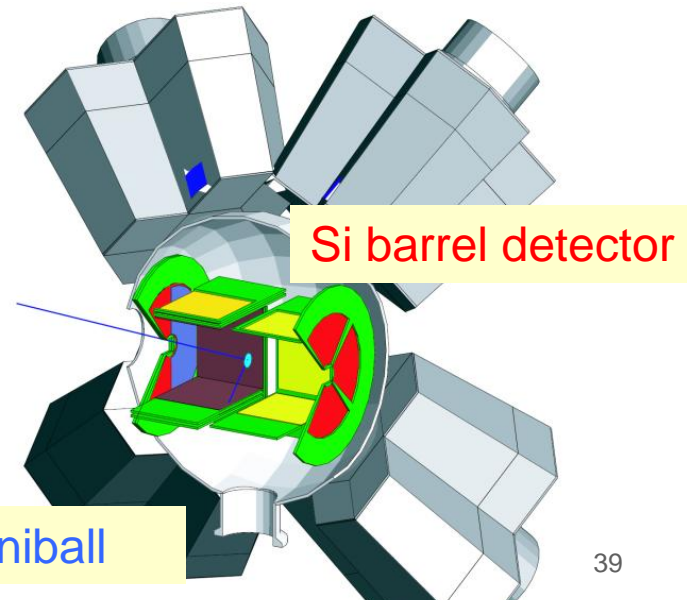
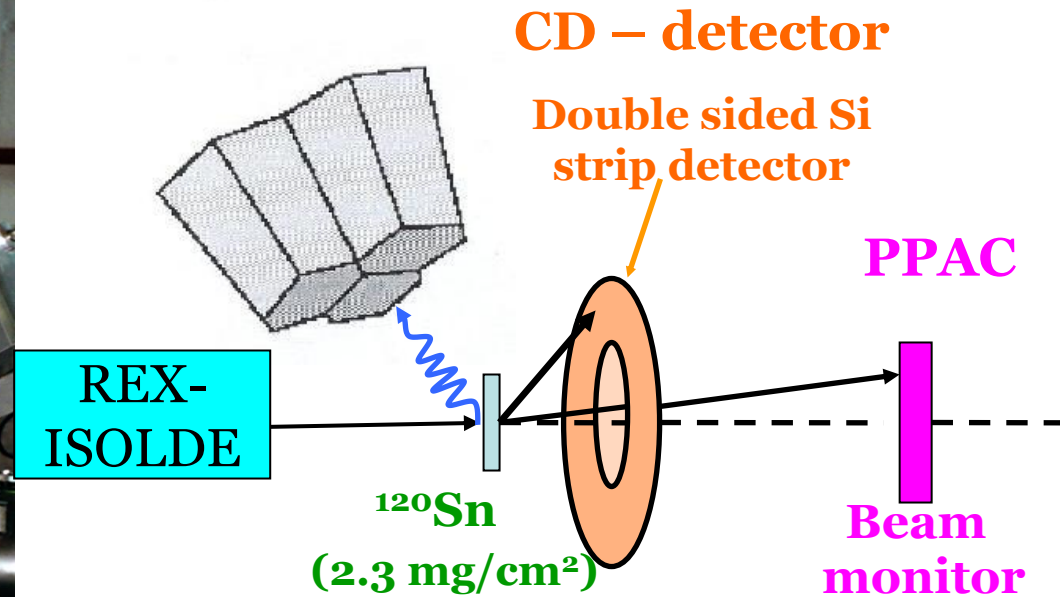
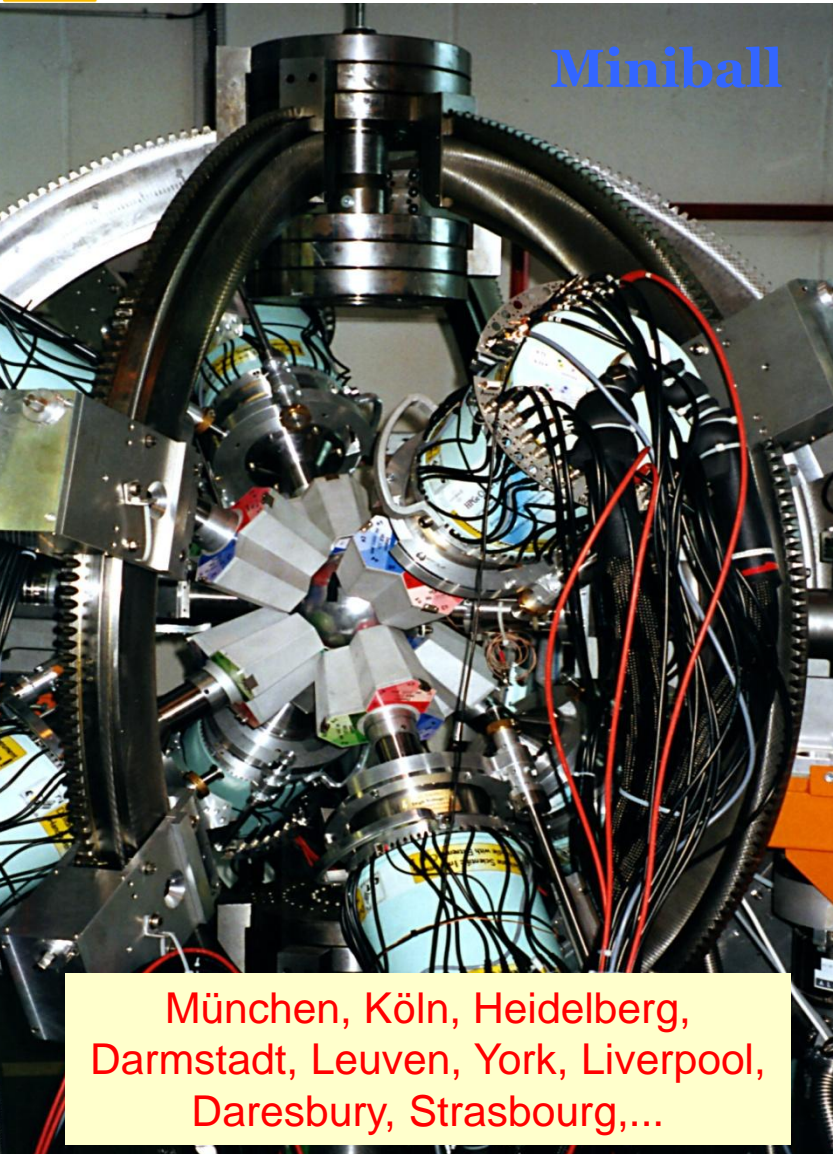
Quadrupole moments (Q_0) in ^{74}Kr and ^{76}Kr



- direct confirmation of the prolate – oblate shape coexistence
- first reorientation measurement with radioactive beam

Coulomb excitation at Rex-Isolde (CERN)

Irfu



J. Eberth et al., *Prog. Part. Nucl. Phys.* 46, 389 (2001)

Wolfram KORTEN

Ecole Joliot

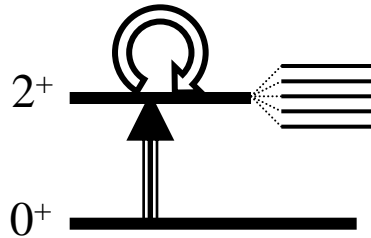
Miniball

Coulomb excitation of ^{70}Se at Rex-ISOLDE

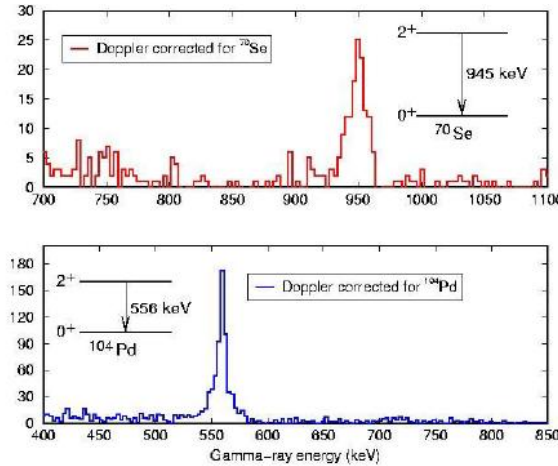
- ^{70}Se on ^{104}Pd at 2.94 MeV/u
- integral measurement
- excitation probability $P(2^+)$ via normalization to known ^{104}Pd

P_{2^+} depends on

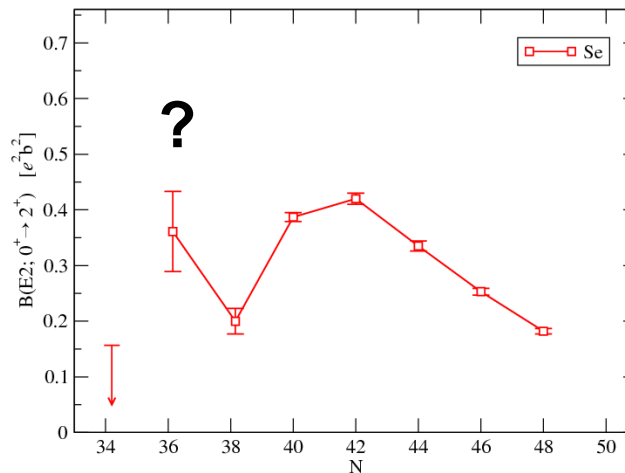
- transitional matrix element $B(E2)$
- diagonal matrix element Q_0



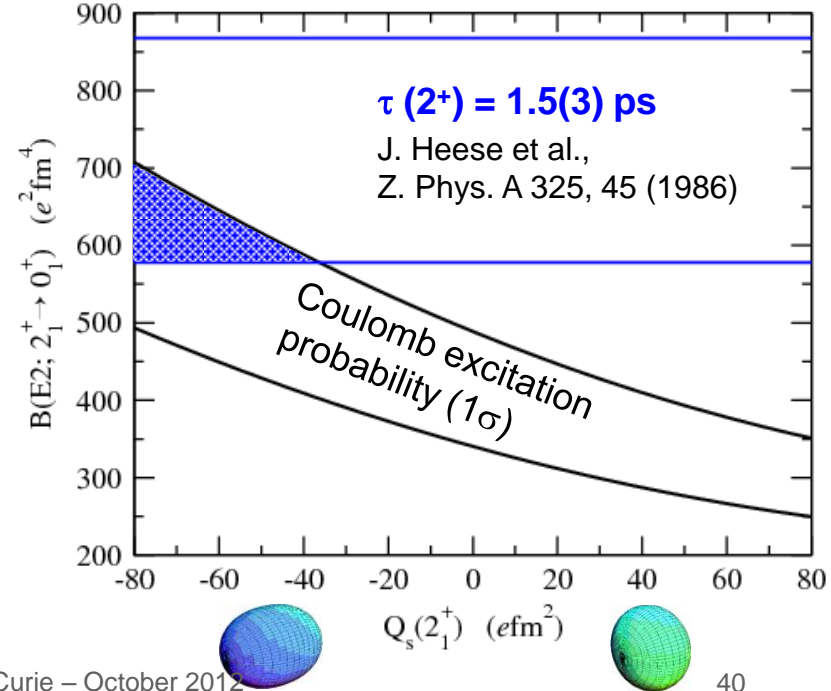
➤ one measurement, but two unknowns !



A.M. Hurst et al., PRL 98, 072501 (2007)
(Univ. Liverpool)



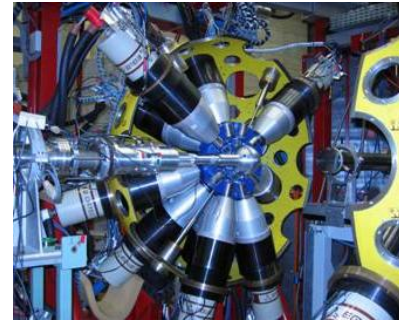
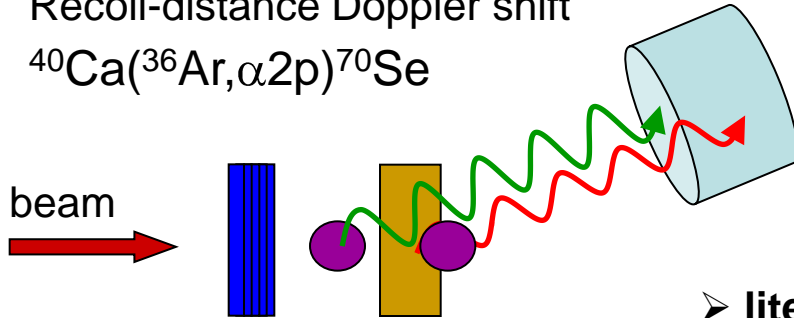
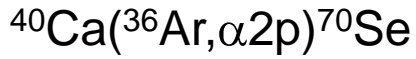
^{68}Se intermediate-energy Coulex GANIL
E. Clément et al., NIM A 587, 292 (2008)



Lifetimes in ^{70}Se revisited

GASP and Köln Plunger at Legnaro

Recoil-distance Doppler shift

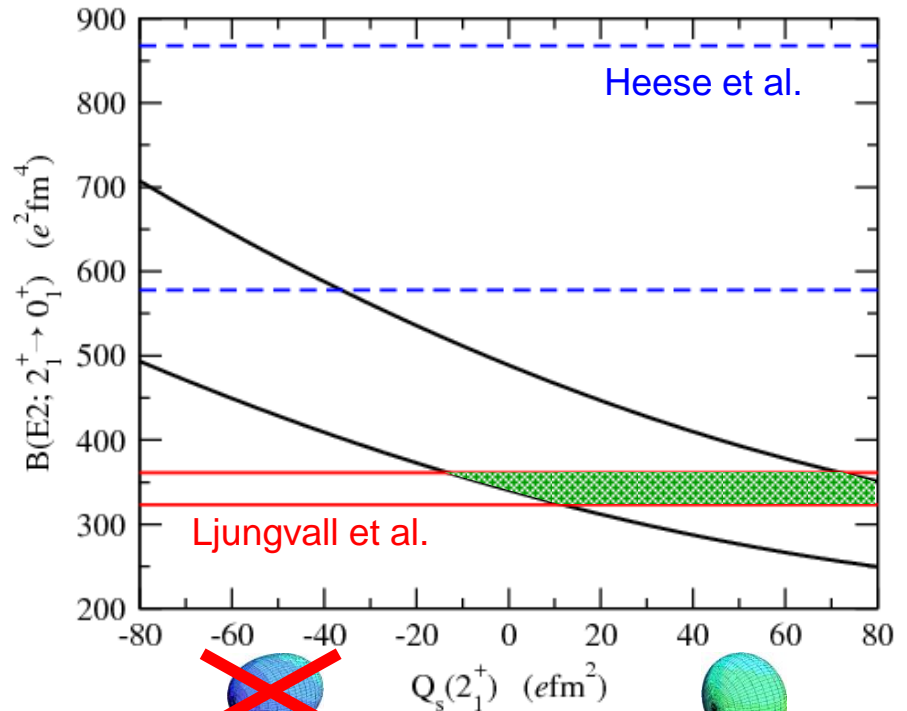
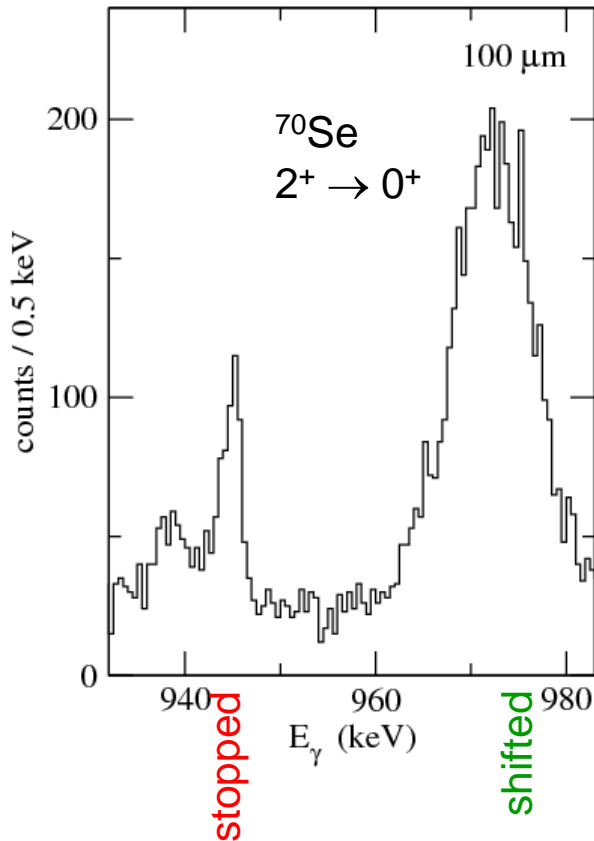


➤ literature value: $\tau = 1.5(3)$ ps

J. Heese et al., Z. Phys. A 325, 45 (1986)

➤ new lifetime for 2^+ in ^{70}Se : $\tau = 3.2(2)$ ps

J. Ljungvall et al., Phys. Rev. Lett. 100, 102502 (2008)



Coulomb excitation of $^{74-80}\text{Zn}$ at Rex-Isolde

^{80}Zn on ^{108}Pd (2.87 MeV/u,
2.0 mg/cm², 3000 pps)

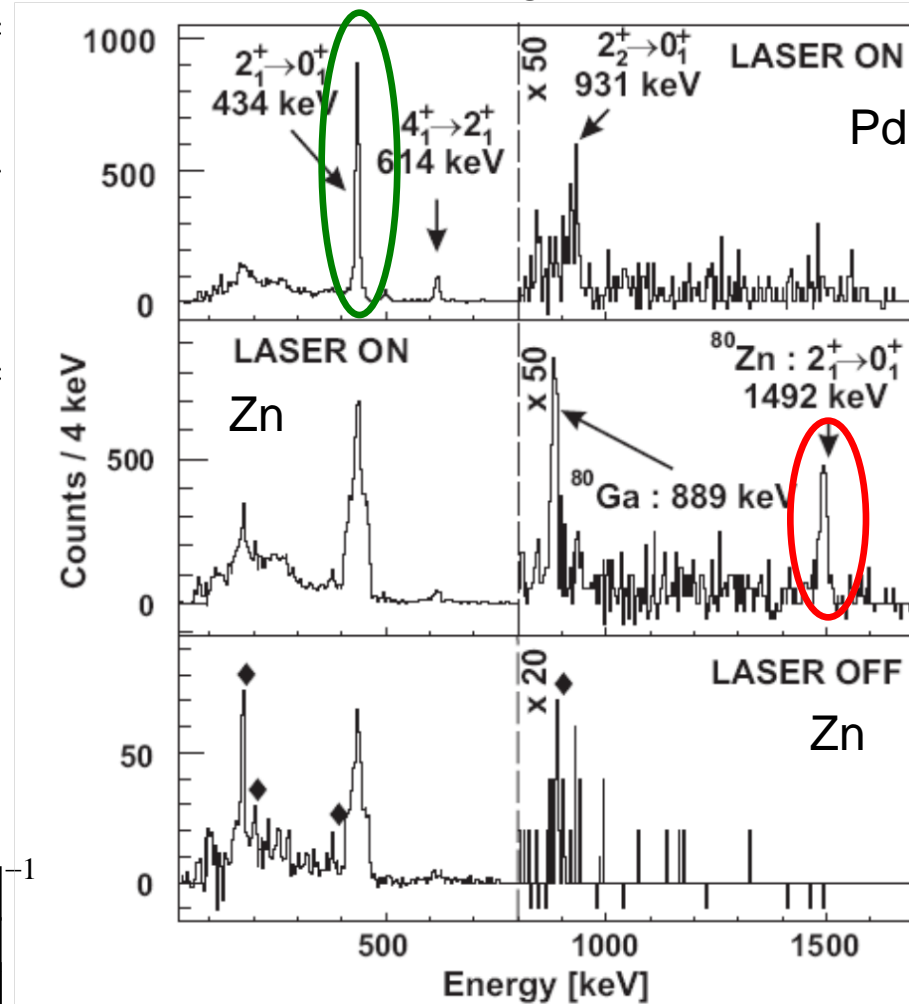
A	$T_{1/2}$ (s)	$f_{\text{Ga}}/f_{\text{Zn}}$ (%)	Zinc beam intensity (ions/s)	
			(1)	(2)
74	95.6(12)	0.1	4.0E7	3.0E5
76	5.7(3)	1.5(1)	1.0E7	1.1E5
78	1.47(15)	5.8(6)	7.8E5	4.3E3
80	0.54(2)	16.2(6)	6.8E4	3.0E3

$$\frac{\sigma(\text{Zn})}{\sigma(\text{Pd})} = \frac{\varepsilon_{\gamma}(\text{Pd}) W_{\gamma}(\text{Pd}) N_{\gamma}(\text{Zn})}{\varepsilon_{\gamma}(\text{Zn}) W_{\gamma}(\text{Zn}) N_{\gamma}(\text{Pd})}$$

Beam contaminants

- increase for more exotic beams
- must be taken into account when calculating the target excitation

$$\frac{N_{\gamma}^{\text{Zn}}(\text{Pd})}{N_{\gamma}^{\text{Tot}}(\text{Pd})} = \left[1 - \left(\frac{f_{\text{Ga}}}{f_{\text{Zn}}} - \frac{I_{\text{Ga}}^S}{f_{\text{Zn}} I^L} \right) \frac{\sigma^{\text{Ga}}(\text{Pd})}{\sigma^{\text{Zn}}(\text{Pd})} \right]^{-1}$$



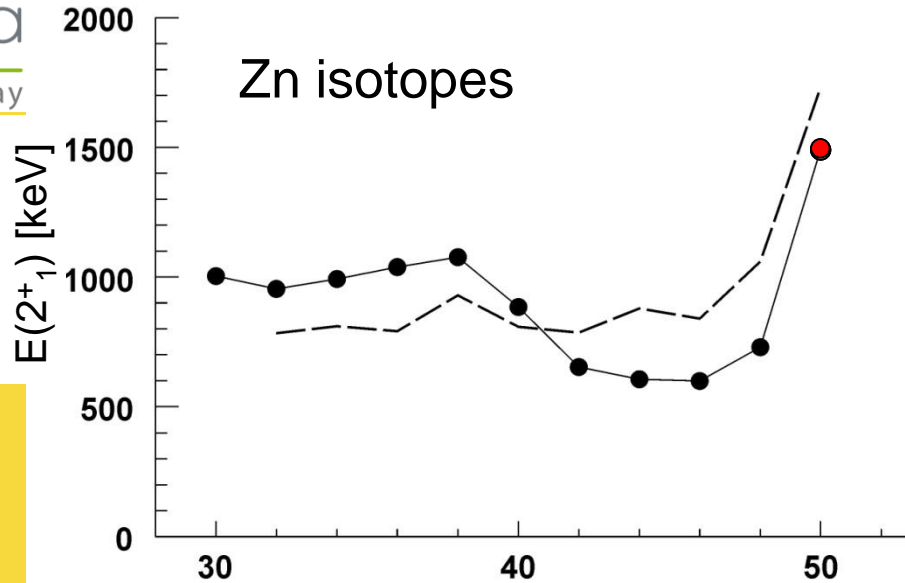
J. Van de Walle et al., PRL 99, 142501 (2007)
and PRC 79, 014309 (2009)

Quadrupole collectivity of the Zn isotopes

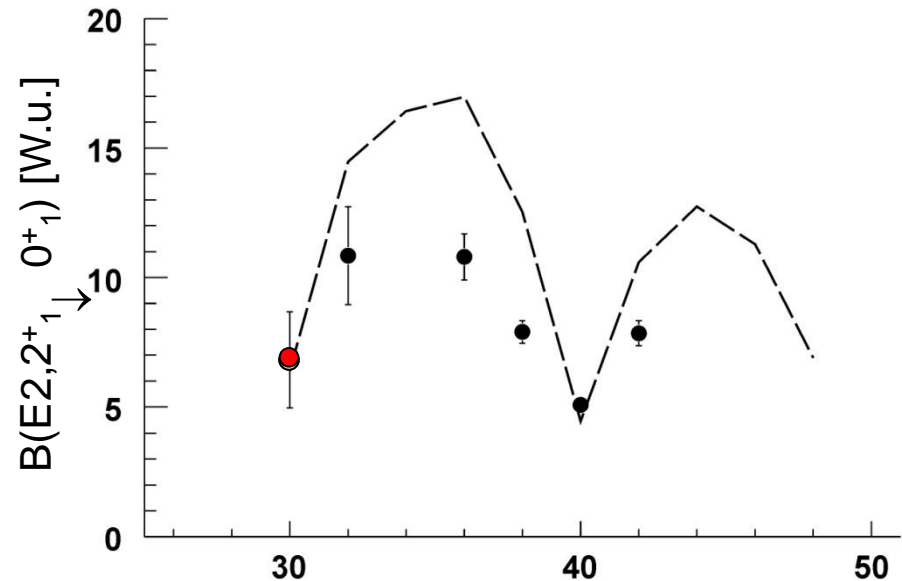
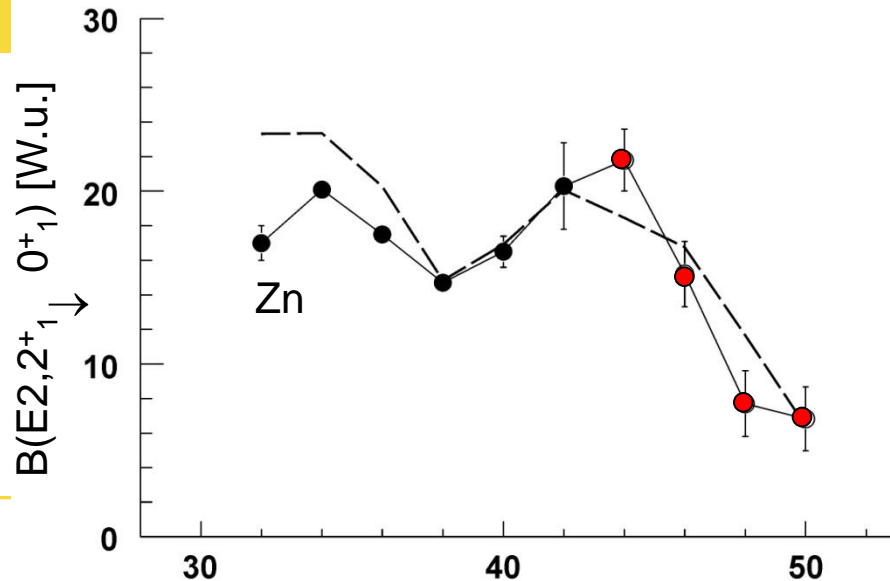
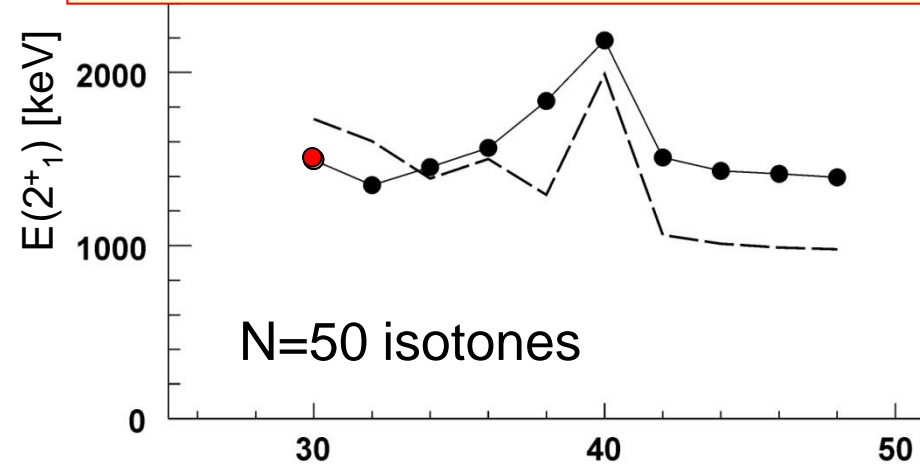
l r f u

cea

saclay



Shell Model (1) ⁵⁶Ni core
 M. H. Jensen + monopole adjusted by F. Nowacki
 (e_{π}, e_{ν}) = (1.9e, 0.9e) – N. Smirnova *et al.*

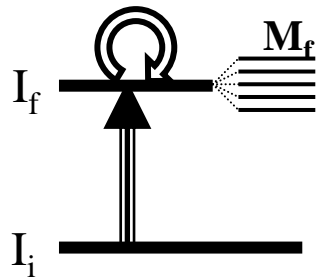
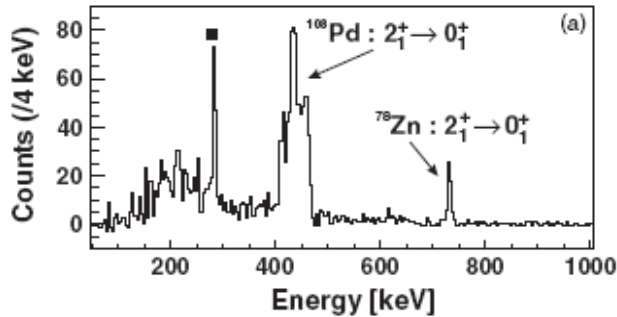


Neutron Number

Proton Number

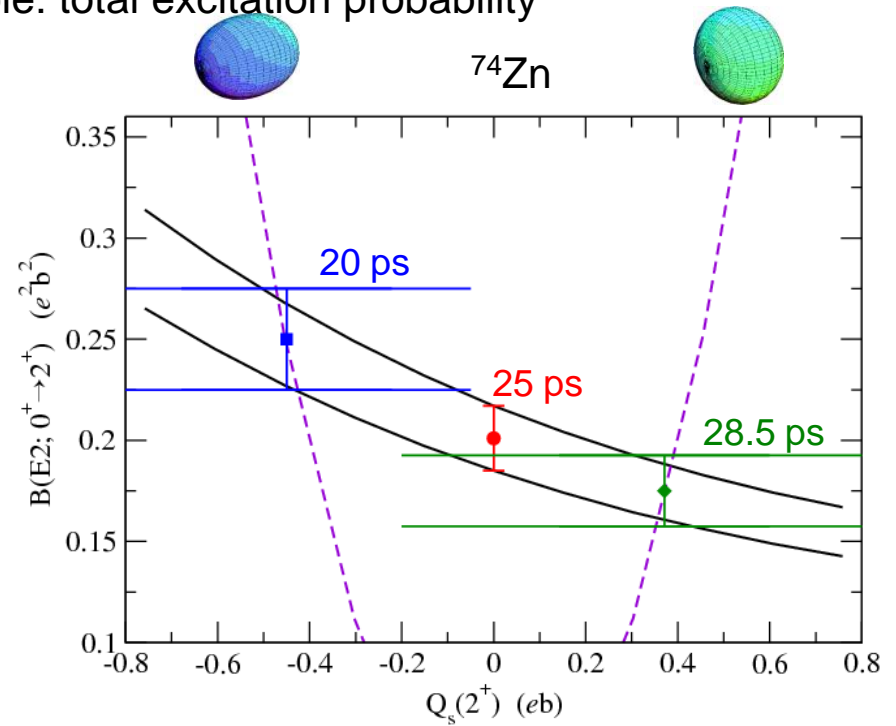
Coulomb excitation of ^{74}Zn at Rex-Isolde

Integral measurement \rightarrow one observable: total excitation probability



two unknowns:

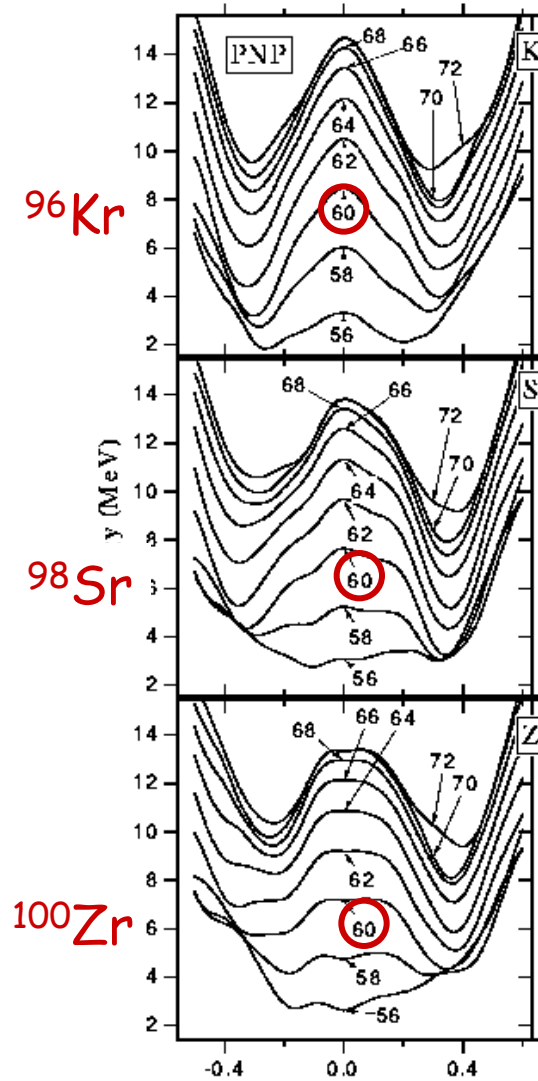
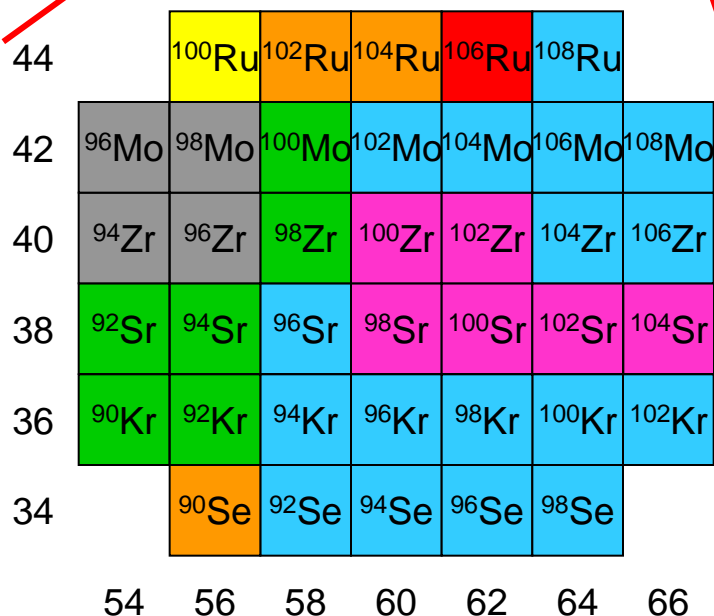
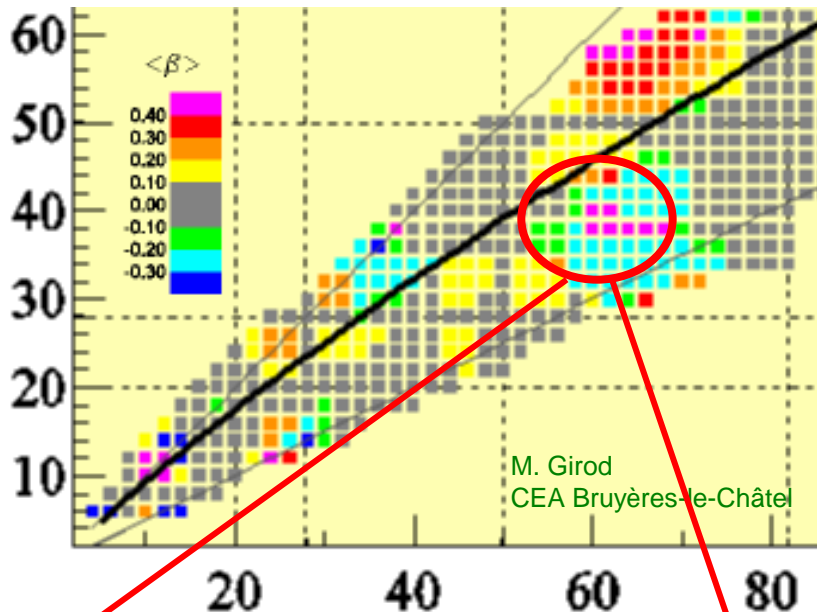
- \blacktriangleright $B(E2)$
- \blacktriangleright Q_s



Life time measurements possible after multi-nucleon transfer reactions by using RDDS technique : reduce $B(E2)$ error and determine Q_0

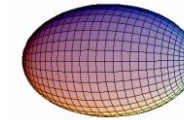
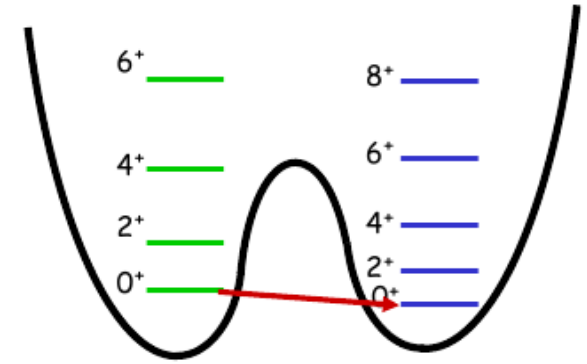
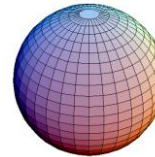
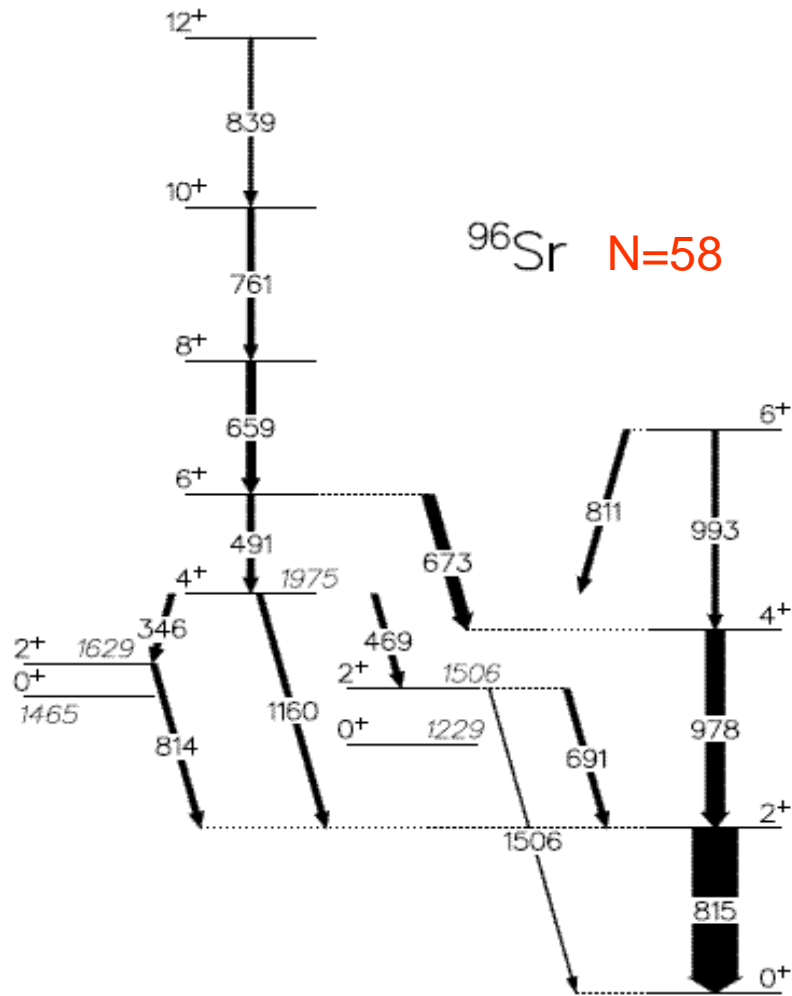
$\tau(2^+) \sim 28.5 \pm 3.6$ ps \rightarrow slight preference for **oblate shape**

Shapes in neutron-rich $A=100$ nuclei

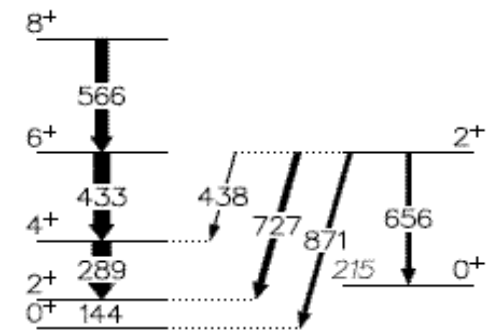


J. Skalski et al., NPA 617, 282 (1997)

Shape transition in Sr isotopes



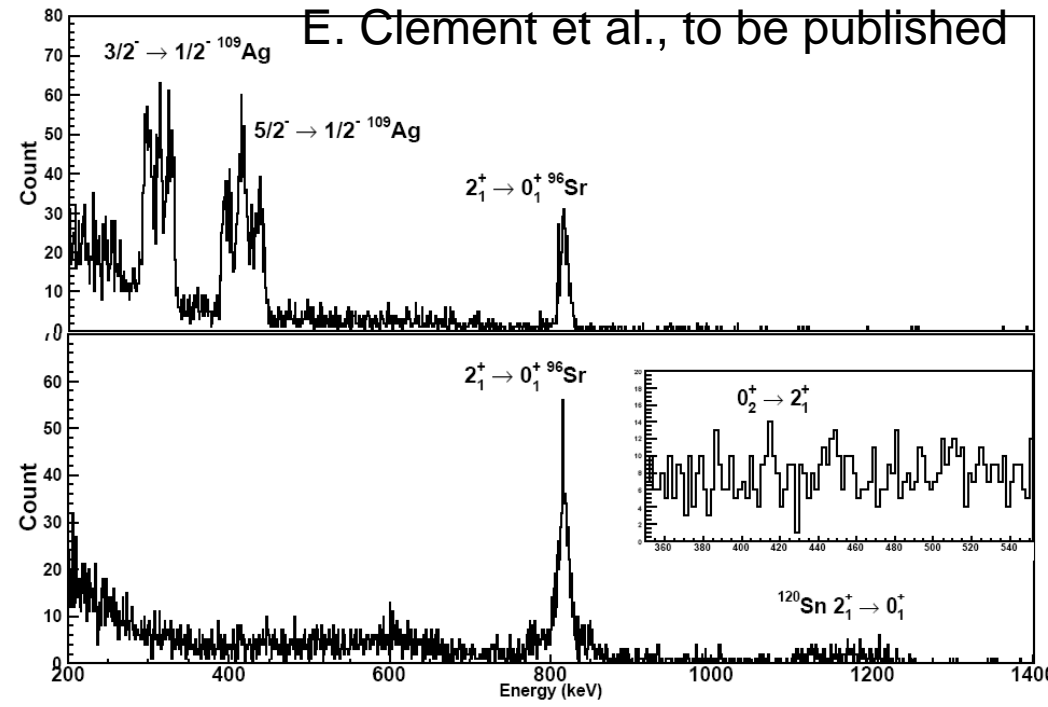
^{98}Sr $N=60$



Coulomb excitation of ^{96}Sr at Rex-Isolde

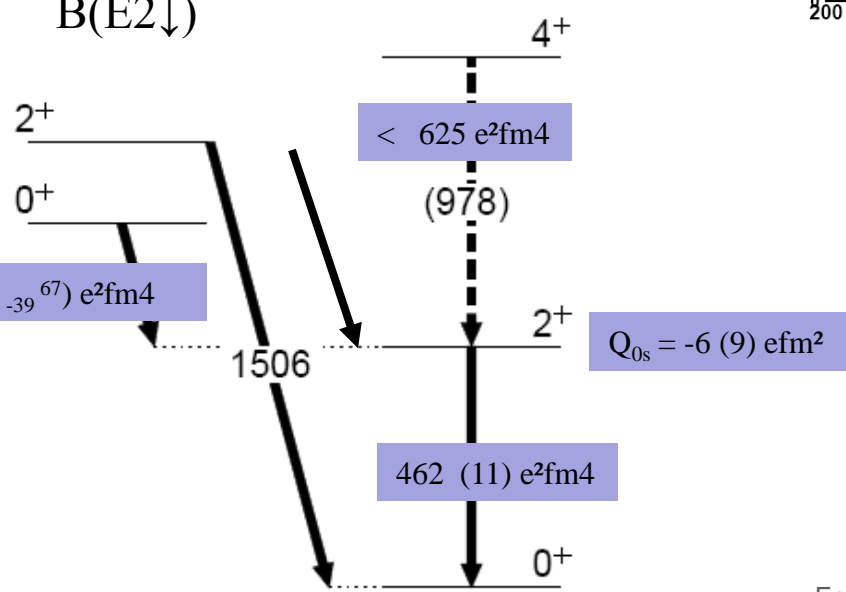
Coulomb excitation on ^{120}Sn and ^{109}Ag

- ☀ Coulex normalisation through the target gamma line
- ☀ Differential and integrated cross section → GOSIA analysis



E. Clement et al., to be published

$B(E2\downarrow)$



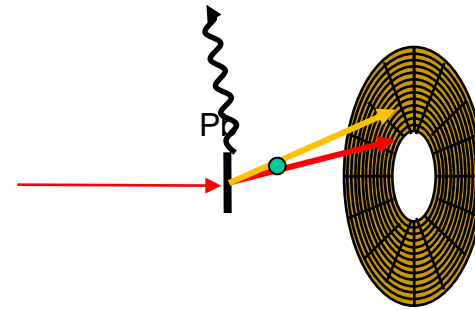
□ The Electric spectroscopic Q_0 is null as its $B(E2)$ is rather large

- Quasi vibrator character
- No quadrupole deformation
- Weak mixing

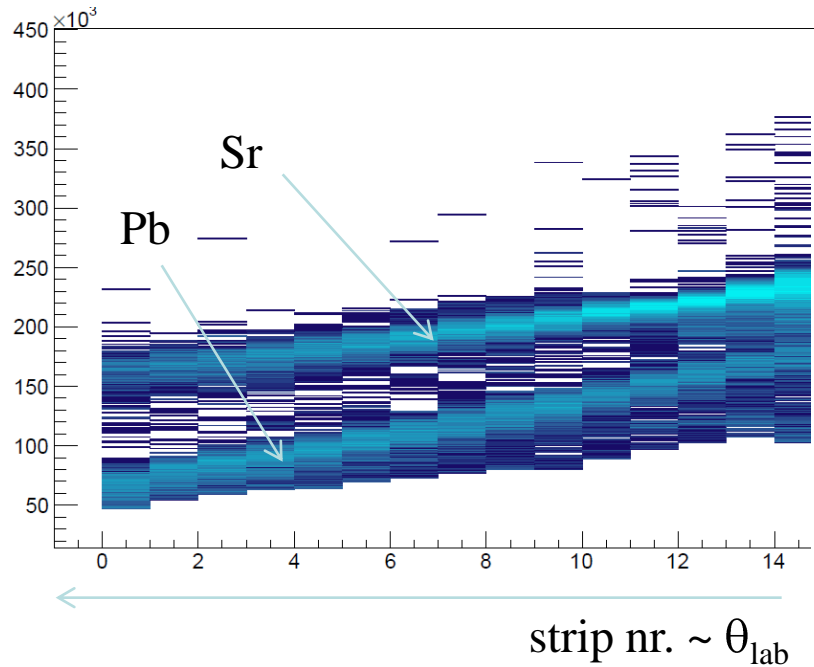
Coulomb excitation results on ^{98}Sr

E. Clement et al., to be published

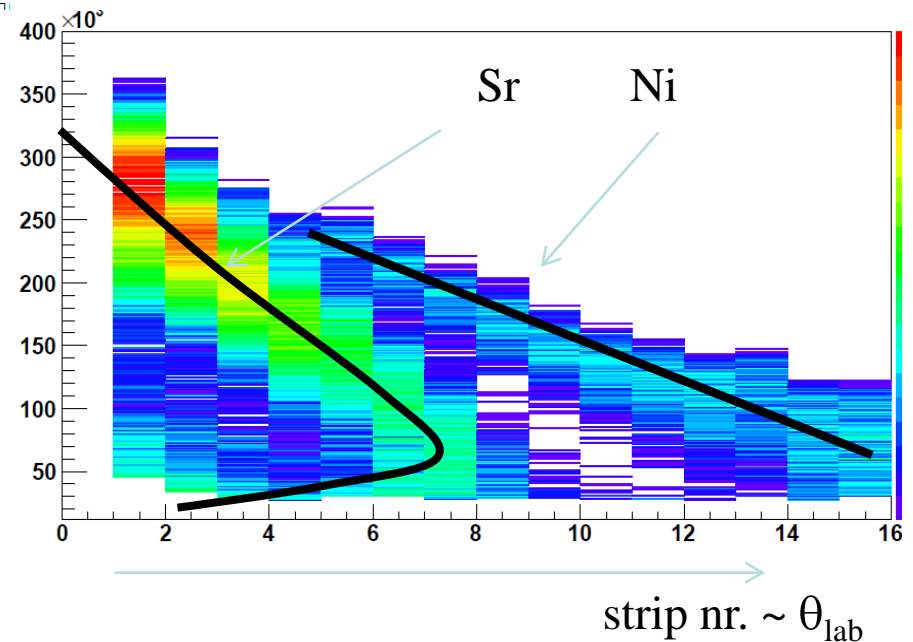
- 2 targets : ^{208}Pb & ^{60}Ni
- clean kinematic separation



^{208}Pb target : direct kinematics

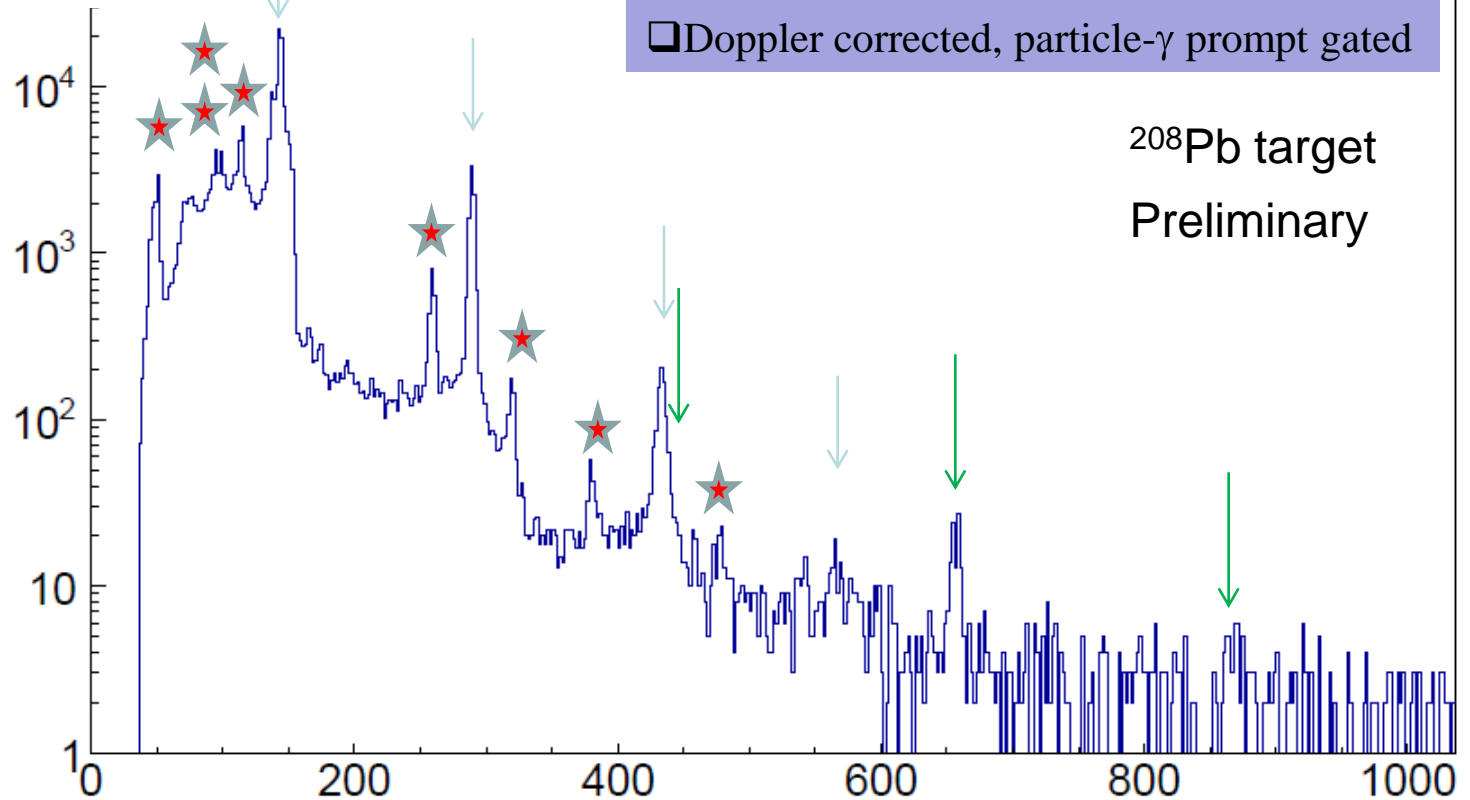
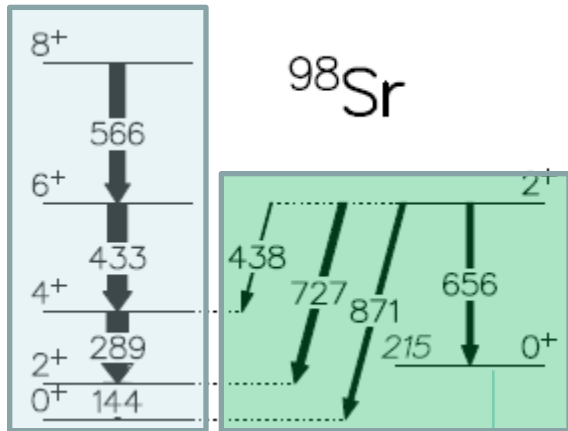


^{60}Ni target: inverse kinematics



Coulomb excitation results on ^{98}Sr

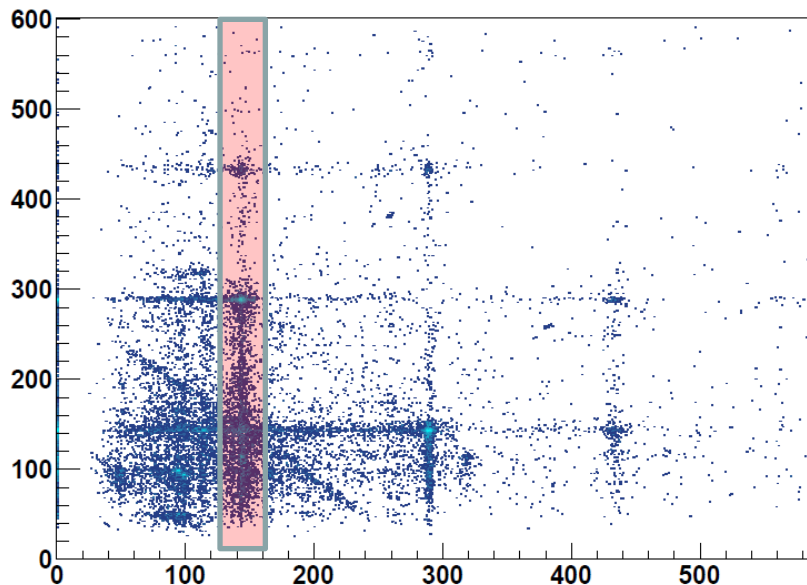
E. Clement et al., to be published



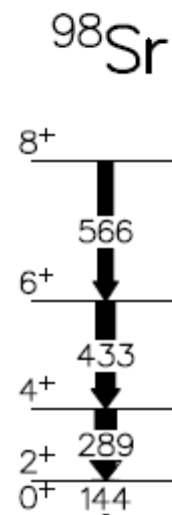
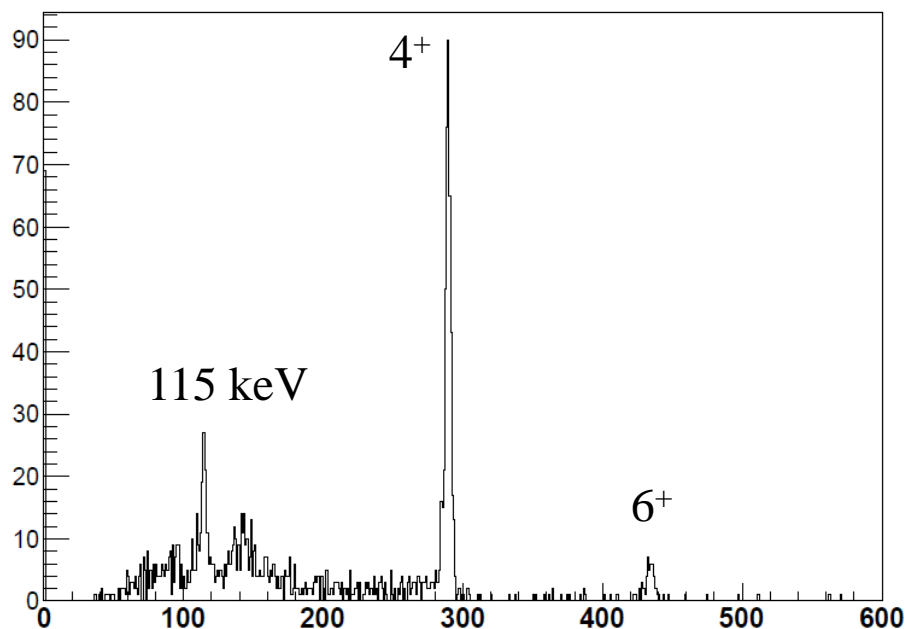
Coulomb excitation on ^{98}Sr (γ - γ analysis)

E. Clement et al., to be published

- ⊙ γ - γ matrix (using RIB)
- ⊙ Many transitions are in coincidence



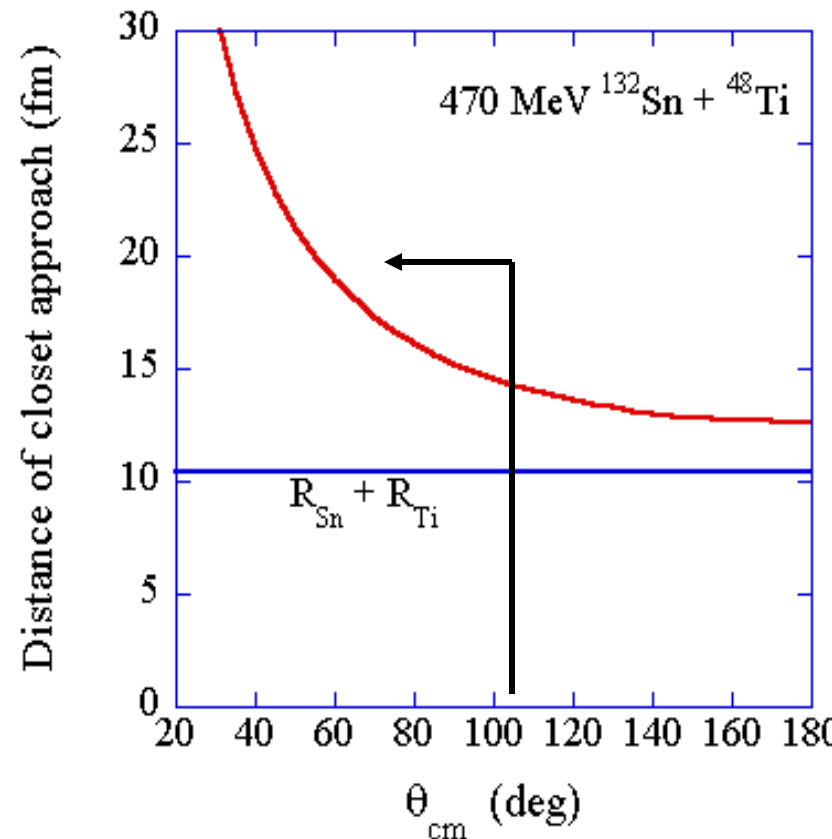
Gated on the 2^+ decay



Coulomb Excitation of ^{132}Sn at HRIBF

- Opportunity to study a new doubly magic nucleus
- Study collectivity of $N=82, Z=50$ core excitation
- High $E(2^+) \sim 4\text{MeV}$ + small $B(E2)$ + weak beam (10^4 pps)
→ very low event rate

- Employ high efficiency BaF_2 γ -array
 - $\sim 40\%$ full-energy at 4 MeV
- Use high-Z target (^{48}Ti)
- Run at higher (“unsafe”) energies (495 MeV and 470 MeV)
- Limit distance of closest approach by looking only at forward angles in center of mass



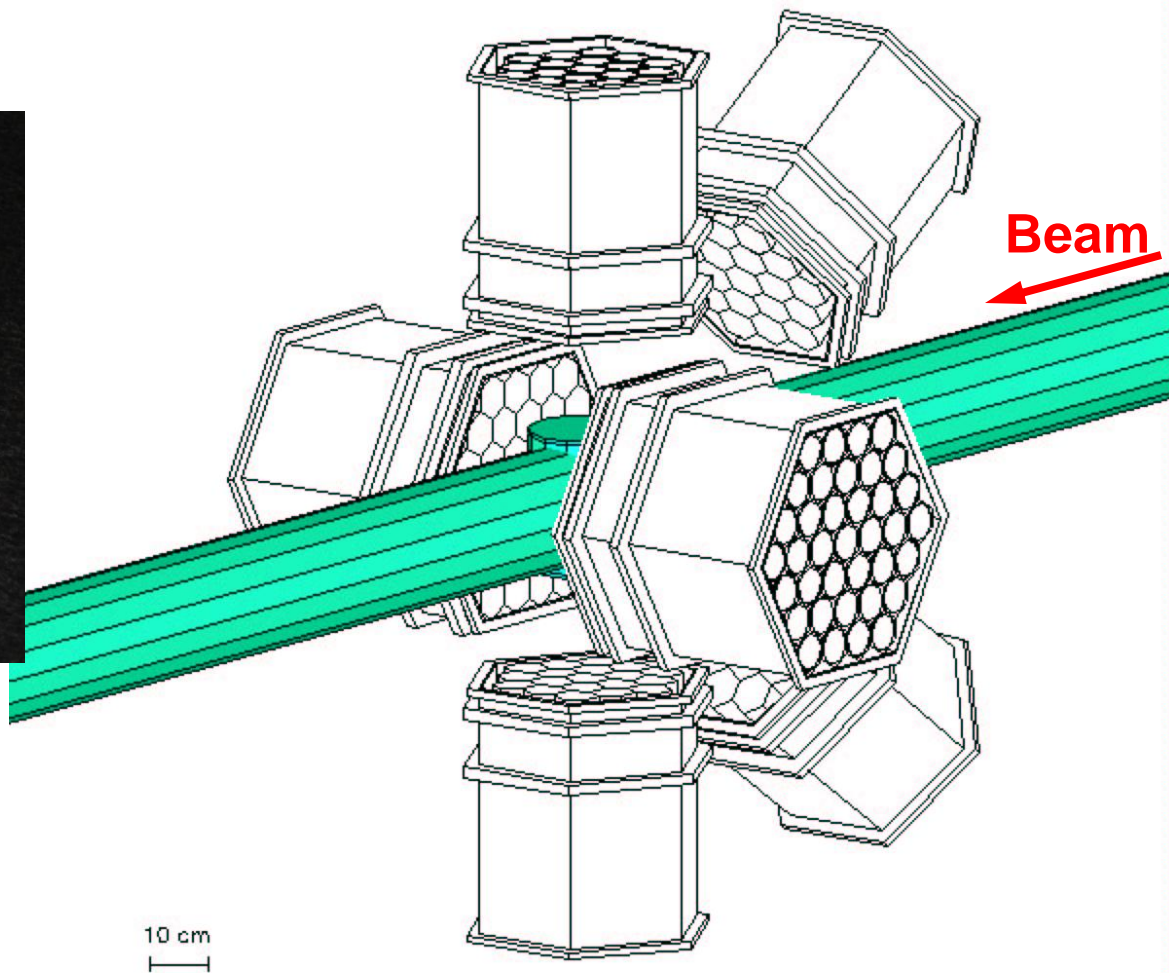
Setup for $^{132,134}\text{Sn}$ Coulomb Excitation

I r f u

cea

saclay

**BaF₂ array (150 crystals)
for gamma-rays**



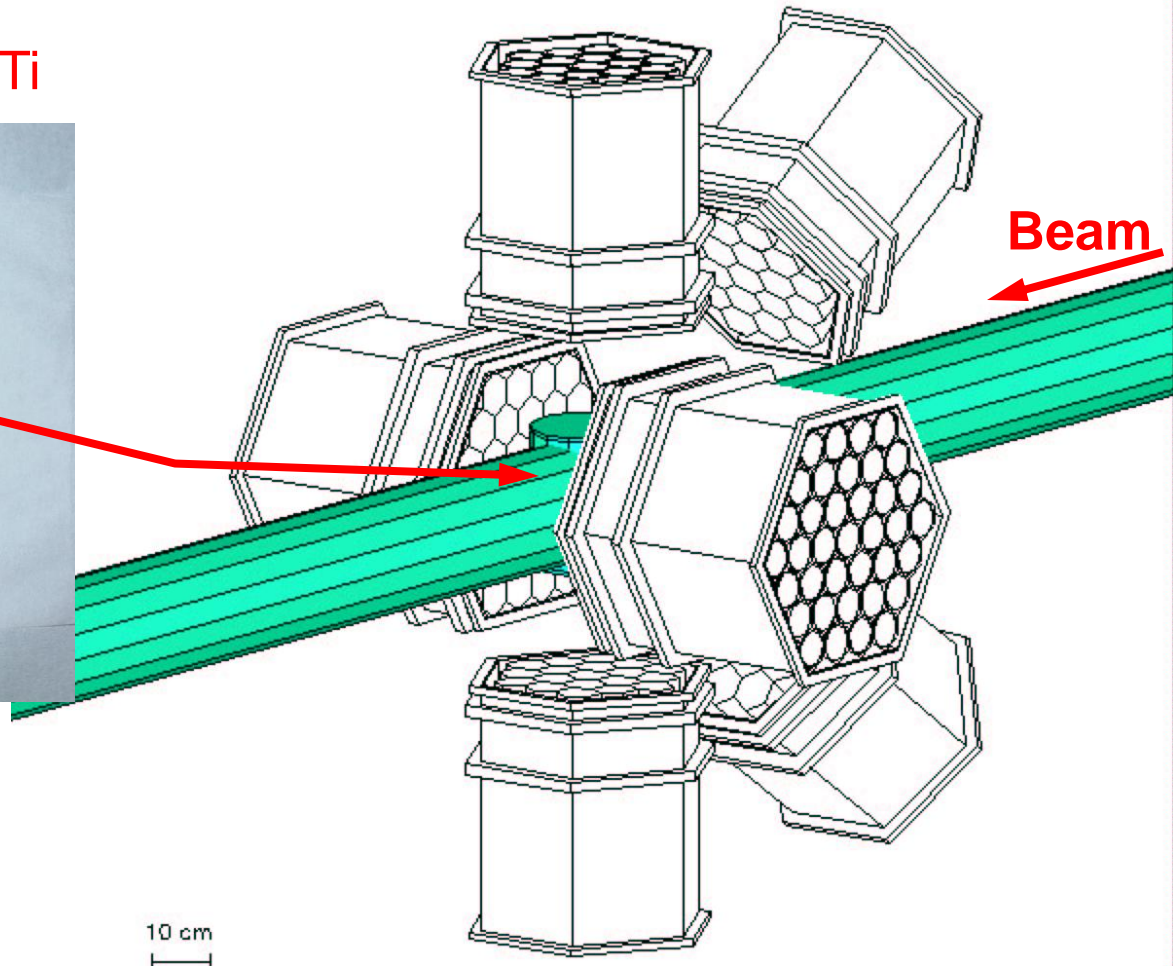
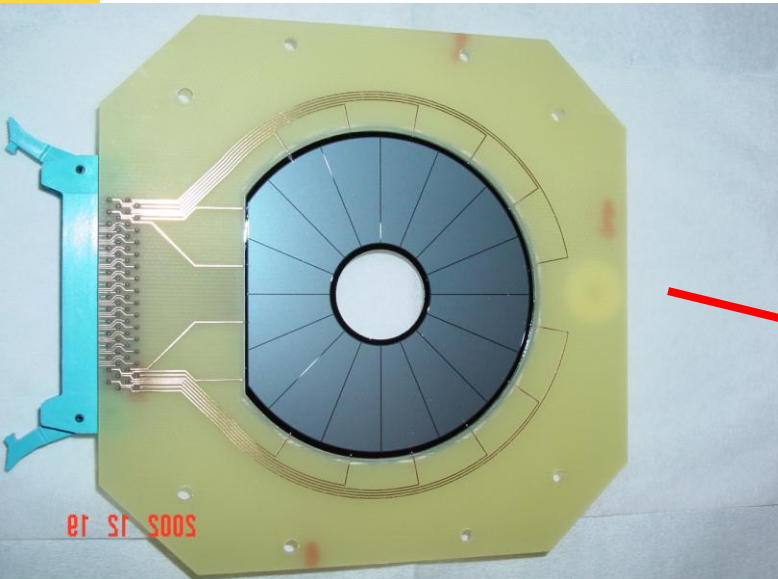
Setup for $^{132,134}\text{Sn}$ Coulomb Excitation

l r f u

cea

saclay

“CD”-type Si detector for scattered Sn and Ti



- 7 cm diameter
- 48 radial strips
- 16 sectors

$$\theta_{\text{LAB}} \sim 7^\circ - 25^\circ$$

$$\theta_{\text{CM}} \sim 30^\circ - 160^\circ$$

Wolfram KORTEN

First results on ^{132}Sn

I r f u

cea

saclay

- ^{132}Sn beam, doubly stripped
 - 96% pure
 - 1.3×10^5 ions/s
 - 3.75 & 3.56 MeV/u
- ^{48}Ti target
- High γ efficiency ($\sim 40\%$)
- Two-week experiment
- Fast γ -ion coincidences to suppress background

First results on ^{132}Sn

l r f u

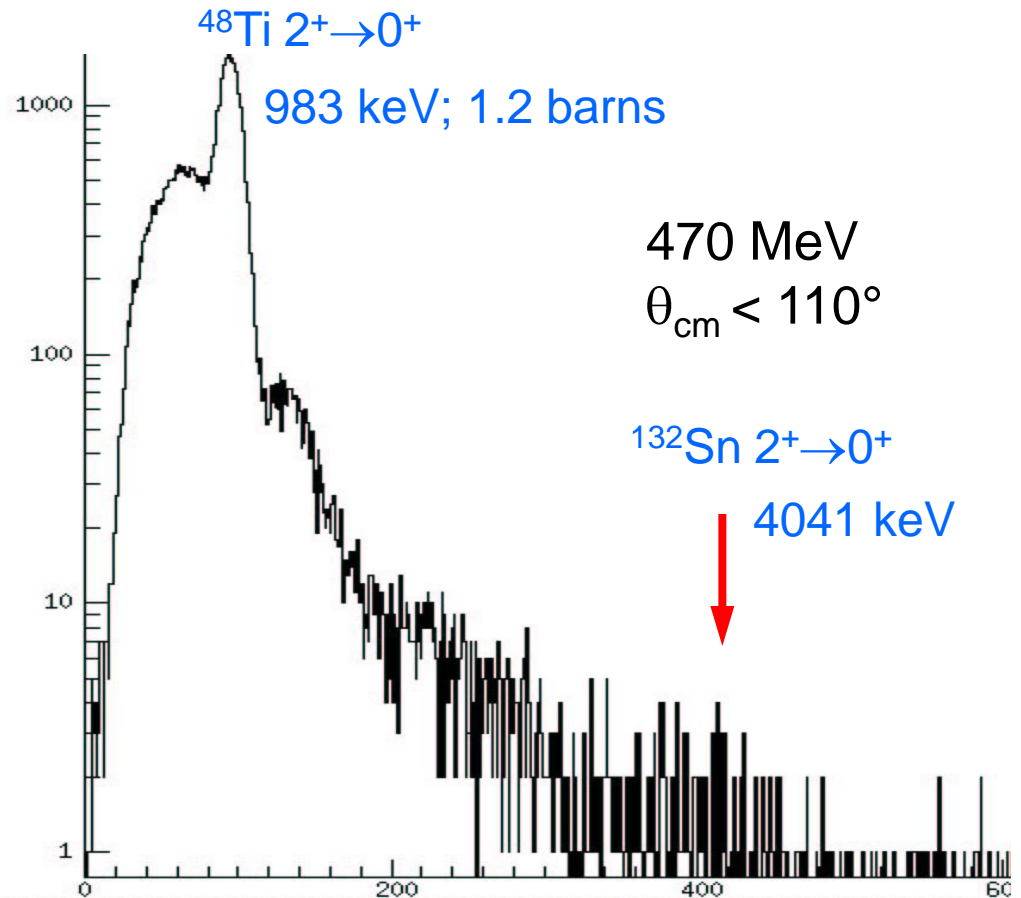
cea

saclay

- ^{132}Sn beam, doubly stripped
 - 96% pure
 - 1.3×10^5 ions/s
 - 3.75 & 3.56 MeV/u
- ^{48}Ti target
- High γ efficiency ($\sim 40\%$)
- Two-week experiment
- Fast γ -ion coincidences to suppress background

Sample gamma-ray spectrum:

- $\sim 30\%$ of data
- Crystal gain matching & background suppression not yet optimum



First results on ^{132}Sn

l r f u

cea

saclay

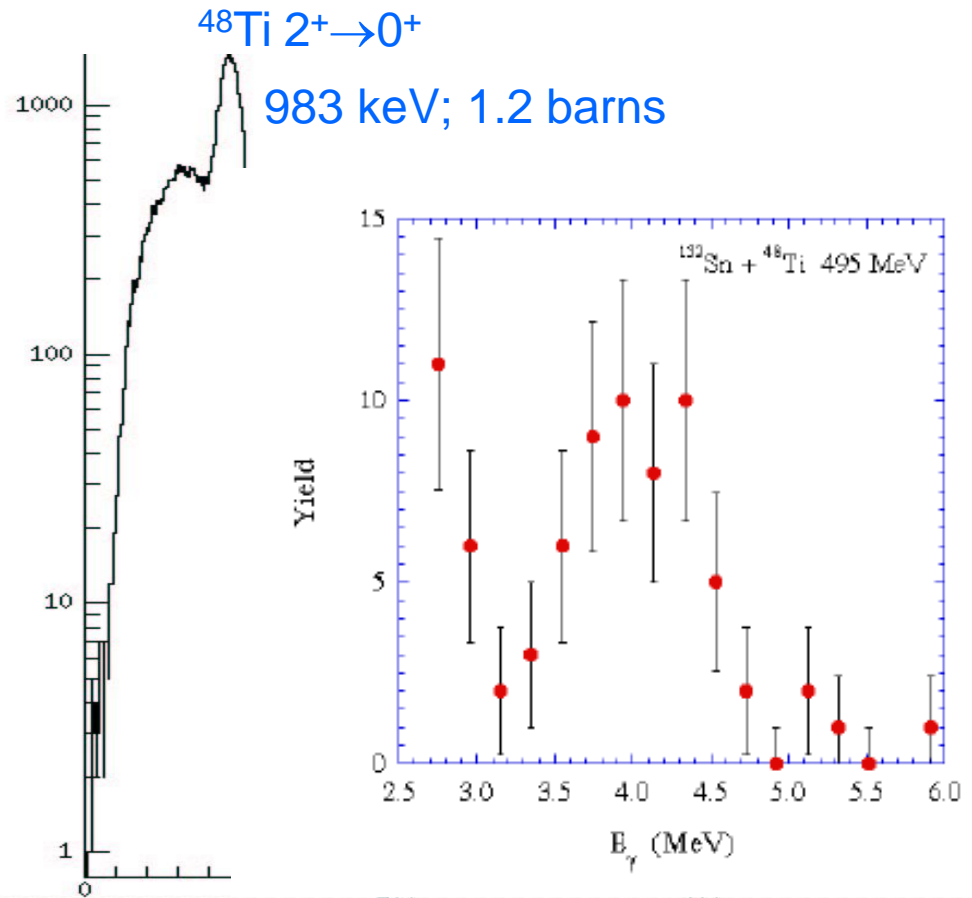
- ^{132}Sn beam, doubly stripped
 - 96% pure
 - 1.3×10^5 ions/s
 - 3.75 & 3.56 MeV/u
- ^{48}Ti target
- High γ efficiency ($\sim 40\%$)
- Two-week experiment
- Fast γ -ion coincidences to suppress background

$B(E2; 0^+ \rightarrow 2^+) \sim 0.11(3) e^2 b^2$

R. Varner *et al.*,
EPJ. A 25, s01, 391 (2005)

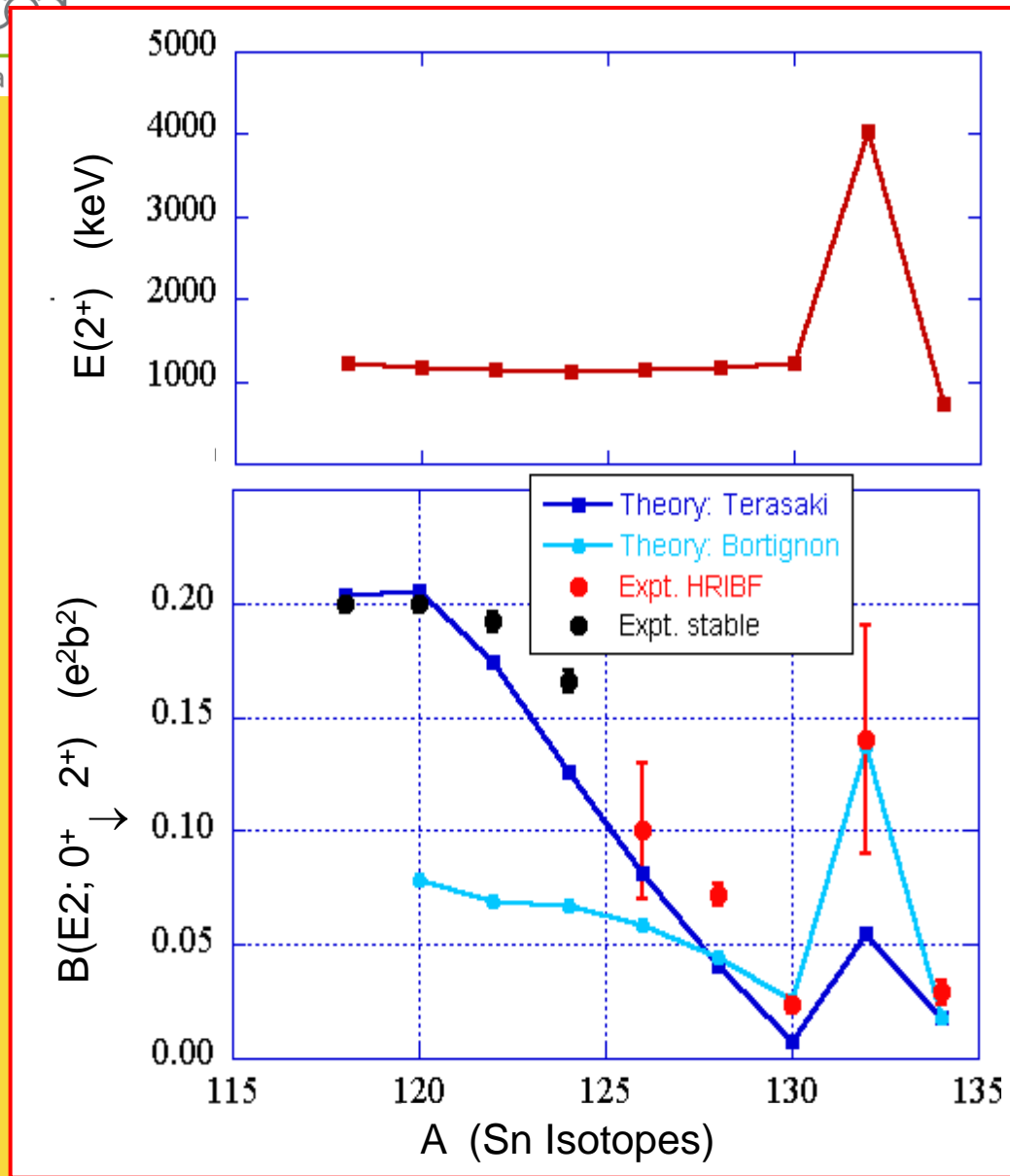
Sample gamma-ray spectrum:

- $\sim 30\%$ of data
- Crystal gain matching & background suppression not yet optimum



Coulomb Excitation Results for Sn isotopes

l r f u
sa



- ^{132}Sn : **$B(E2) \sim 0.11(3) e^2b^2$**
 - 14% Isoscalar E2 EWSR
- ^{134}Sn : **$B(E2) = 0.029(5) e^2b^2$**

New facilities needed in order to fully explore this mass region

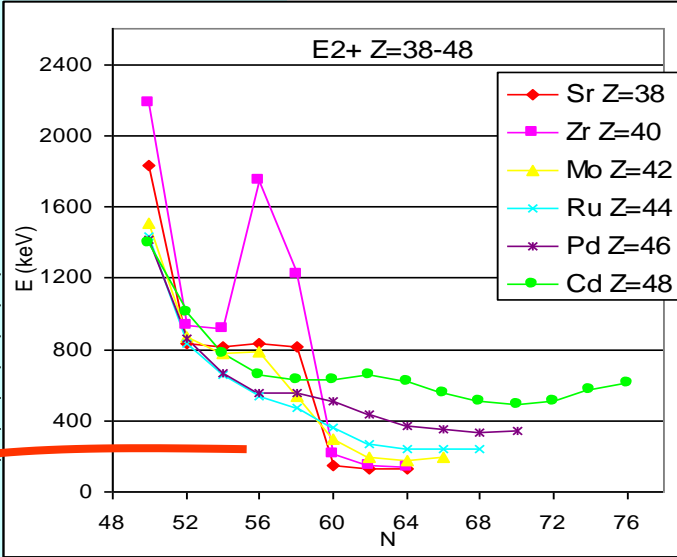
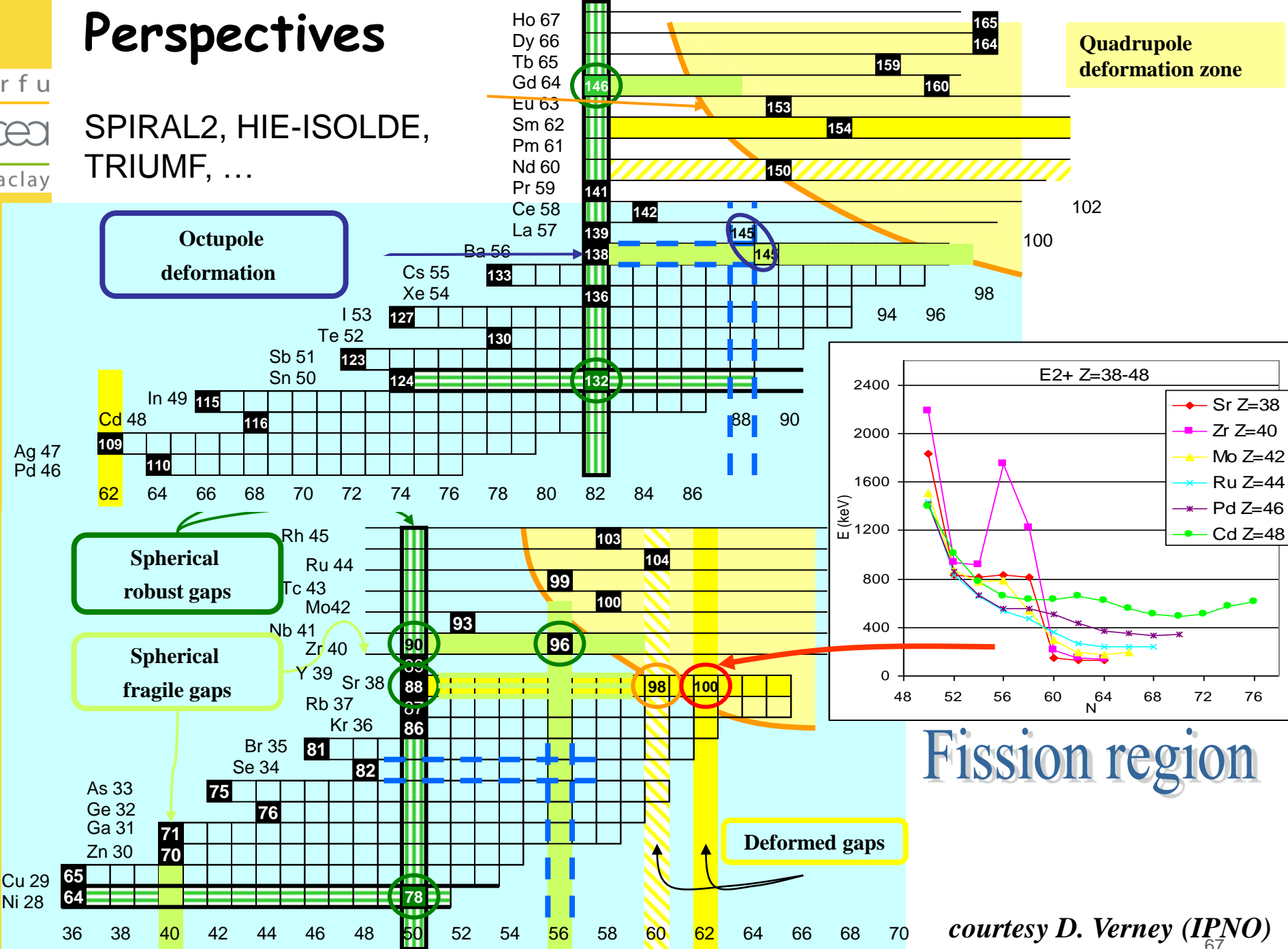
Perspectives

Ir fu

cea

saclay

SPIRAL2, HIE-ISOLDE,
TRIUMF, ...



Coulomb excitation studies with low-energy RIBs

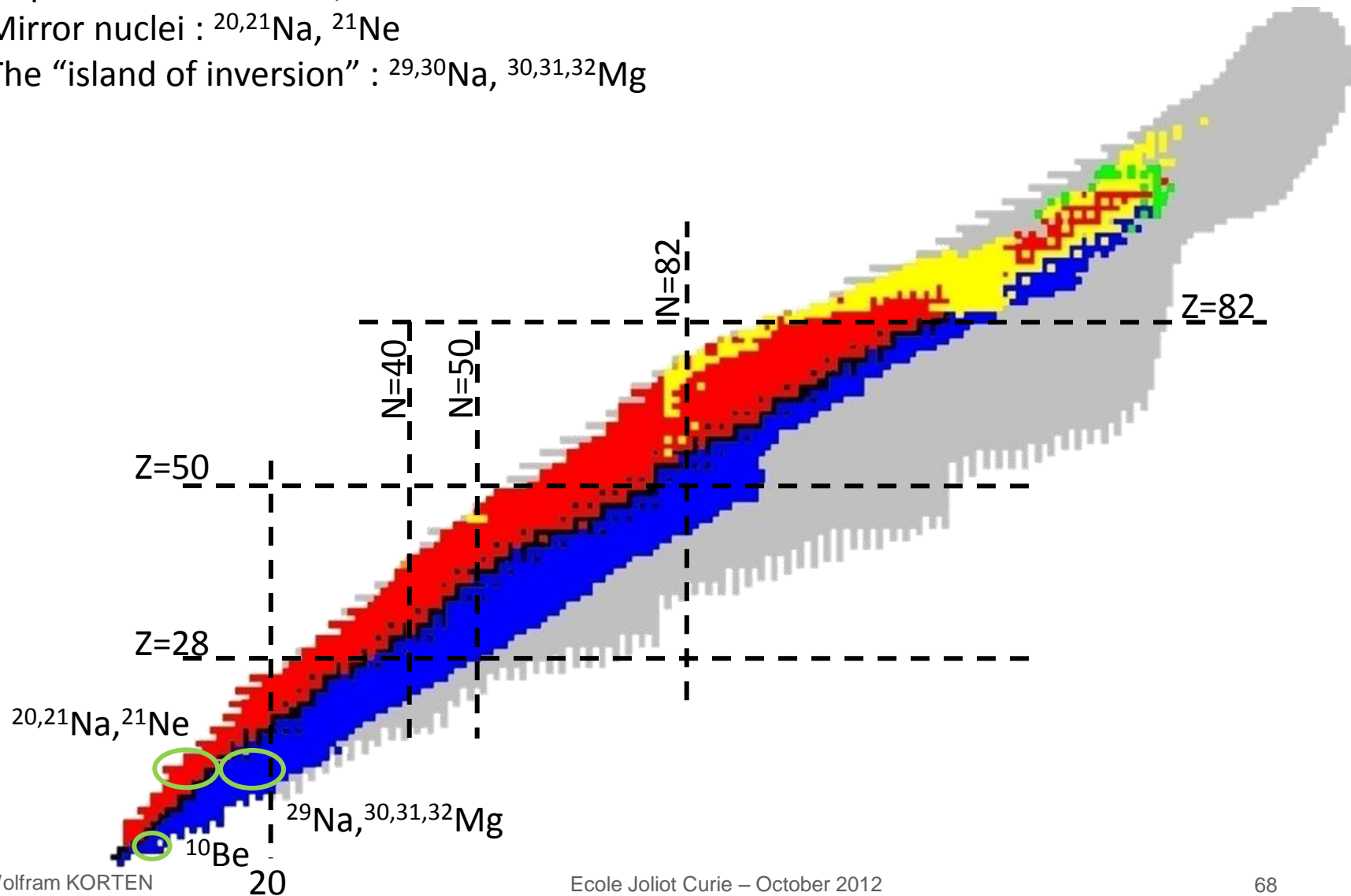
I r f u

cea

saclay

Drip lines and shell structure in light nuclei

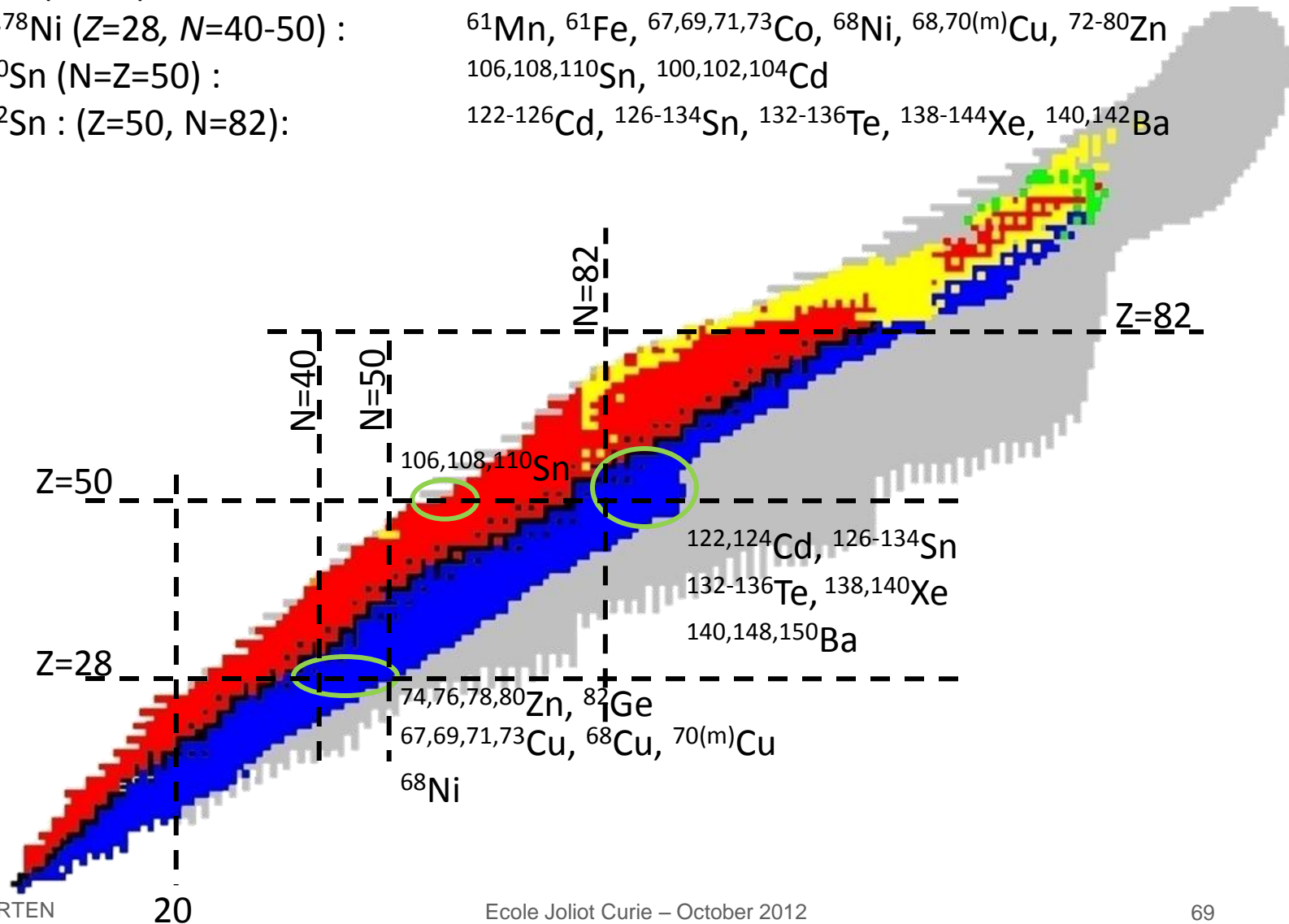
- ✓ Drip-line nuclei: $^{10,11}\text{Be}$, ...
- ✓ Mirror nuclei : $^{20,21}\text{Na}$, ^{21}Ne
- ✓ The “island of inversion” : $^{29,30}\text{Na}$, $^{30,31,32}\text{Mg}$



Coulomb excitation studies with low-energy RIBs

Evolution of Shell Structure far from stability

- ✓ ^{44}Ar (N=28)
- ✓ $^{68,78}\text{Ni}$ (Z=28, N=40-50) : ^{61}Mn , ^{61}Fe , $^{67,69,71,73}\text{Co}$, ^{68}Ni , $^{68,70(m)}\text{Cu}$, $^{72-80}\text{Zn}$
- ✓ ^{100}Sn (N=Z=50) : $^{106,108,110}\text{Sn}$, $^{100,102,104}\text{Cd}$
- ✓ ^{132}Sn : (Z=50, N=82): $^{122-126}\text{Cd}$, $^{126-134}\text{Sn}$, $^{132-136}\text{Te}$, $^{138-144}\text{Xe}$, $^{140,142}\text{Ba}$



Coulomb excitation studies with low-energy RIBs

l r f u

cea

saclay

Evolution of nuclear shapes and shape coexistence

- ✓ $N=Z \approx 34$: ^{70}Se , $^{72,74,76}\text{Kr}$,
- ✓ $N \approx 60$: $^{88-96}\text{Kr}$, $^{96,98}\text{Sr}$, $^{93-99}\text{Rb}$, ...
- ✓ $N \approx 82$: ^{140}Nd , $^{140,142}\text{Sm}$
- ✓ $Z \approx 82$: $^{182-188}\text{Hg}$, $^{186,188,200}\text{Pb}$, $^{196-202}\text{Po}$, $^{202,204}\text{Rn}$, ...

